JOURNAL OF COMPUTATIONAL PHYSICS 42, 152–194 (1981)

An Algorithm for Multidimensional Combusting Flow Problems

EDWARD J. KANSA*

United States Bureau of Mines, P.O. Box 18070, Pittsburgh, Pennsylvania 15236

Received November 12, 1979; revised January 22, 1981

An algorithm has been developed for handling the difficulties encountered in modeling subsonic combusting flow problems such as the disparity of timescales, and the highly nonlinear processes such as radiation, turbulence, and exothermic Arrhenius chemical kinetics. This scheme is an extension of the block implicit (BI), Douglas–Gunn ADI scheme modified to include the basic strategies of the stiff ODE and nonlinear equation solvers. For a given time step, the nonlinear finite difference equations are iteratively solved by a linear combination of a damped Newton–Raphson and steepest descent method. Even though the BI method is, without source terms, unconditionally stable according to linear theory, sufficiently large source terms arising from exothermic chemistry may render such a scheme only relatively stable. The time step acts as a damping parameter for a Newton scheme which is adjusted accordingly for solution trajectories in regions of high as well as mild nonlinearity. This algorithm reduces identically to the Briley–McDonald and Beam–Warming noniterative BI scheme if the solution trajectory is sufficiently linear. Iteration is only used if the norm of the residual errors of the finite difference equations exceeds a given tolerance. This algorithm has been applied to coal dust flames and the burning fuel wick problem with and without the influence of the gravitational acceleration. Even though the combustion chemistry is oversimplified, the physics appears to be properly modeled because there is excellent qualitative and quantitative agreement of the calculations with experimental observation.

I. INTRODUCTION

Mathematical effort in combusting fluid flow has been limited due to the numerical difficulties associated with the highly nonlinear processes such as Arrhenius chemical kinetics, radiation, and turbulence superimposed upon fluid flow. Traditional explicit schemes [1, 2] become inefficient in typical combustion problems because the stability requirement is more stringent than the accuracy requirement.

The approach taken in this paper is to combine the best features of the block implicit (BI)-ADI partial differential equation (PDE) scheme with the best features of the stiff ordinary differential equation (ODE) schemes and the damped Newton–Raphson and steepest descent nonlinear equation schemes. The resulting

* Present address: L-451, Lawrence Livermore National Laboratory, P.O. Box 808, Livermore, Calif. 94550.

0021-9991/81/070152-43$02.00/0

algorithm for the highly nonlinear PDEs for combustion problems is very robust and efficient over a very wide range of phenomena.

The paper is organized in the following manner. Section II will present a review of implicit PDE schemes applied to combustion phenomena, showing the evolution of thought up to the present method. Section III presents an outline of the finite difference scheme used in this paper. Section IV first reviews the standard BI-ADI scheme, and then extends it by incorporating it with the principal features of the stiff ODE schemes. Section V discusses the necessity for dynamic time step control for robustness and optimal efficiency.

In Section VI, the problem of attaining the deterministic physically realizable solution among the multiple solutions possible from the nonlinear PDEs is discussed. Section VII discusses computational efficiency questions for treating the detailed chemistry of flames. Finally, Section VIII presents the results of a numerical simulation of a two-dimensional burning wick problem in a gravitational field as the system evolves from ignition to steady state.

II. Review of Combustion Gasdynamic Schemes

Most of the developmental work in the numerical solution of multidimensional PDEs has had direct application to aerospace problems. This section will trace the evolution of thought as successive improvements have been made in combining well proven gasdynamic schemes with combustion.

The ICE scheme of Harlow and Amsden [3] has been the basis of several implicit multidimensional methods. In this method, the mass and momentum conservation equations are solved iteratively as a set of coupled equations by the method of successive substitutions (MSS). The RICE [4, 5] and APACHE [6] codes which are stablized by various forms of truncation error cancellation are codes based on the ICE scheme used for combusting flows. One of the primary disadvantages of the APACHE [6] code is that the iteration scheme is terminated after an upper iteration bound is reached whether or not convergence is achieved.

Westbrook [7] modified the ICE and RICE methods to handle strongly exothermic chemical reactions. Instead of using the adiabatic pressure corrections of the RICE code, he modified the pressure corrections to include temperature and composition changes. In his opinion, during highly exothermic combustion, the corrections due to energy and composition must be solved simultaneously with the mass and momentum corrections.

Keller [8] first proposed using an implicit Newton–Raphson scheme for solving the two point boundary value problem for systems of nonlinear ODEs. Later, he [9, 10] extended this scheme to systems of nonlinear PDEs. The method of Baum and Nfedo [11] utilizes a quasilinear iteration scheme for solving two-dimensional fluid flow problems in the context of a Peaceman–Rachford ADI scheme.

Briley and McDonald [12] and Beam and Warming [13] developed a noniterative block implicit scheme for treating multidimensional compressible flow conservation

equations. Such a scheme permits time steps corresponding to the convective transport time across a computational cell and has overcome the CFL [1, 2] sound speed restriction by treating the pressure gradients and convective transport terms simultaneously and implicitly. The scheme is linearized by a first-order Taylor series expansion about the solution at the known time level to produce a set of coupled linear FDEs. The Douglas–Gunn [14] consistently split alternating direction implicit (ADI) procedure reduces a multidimensional problem to a sequence of one-dimensional problems. This procedure gives rise to a set of coupled linear equations in block tridiagonal form which can be solved by block elimination methods, cf. Keller [8]. Gibeling *et al.* [15] developed MINT, a 3-D Navier–Stokes code with equilibrium chemistry based on the BI-ADI scheme developed by Briley and McDonald [12].

Within a given PDE time step, some chemical reactions may proceed with very little influence on either transport or chemical enthalpy production. That is, the timescales of the Arrhenius kinetics and the transport are sufficiently disparate that, to a good approximation, transport is essentially frozen within the PDE time step. If this is the case, then a time splitting strategy is quite appropriate as recommended by Oran *et al.* [16] and Rivard *et al.* [5]. Under the assumption that transport may be frozen at the old time step value, the PDEs may be rearranged as a system of coupled inhomogeneous ordinary differential equations (ODEs) depending on the problem under consideration, either an analytical or a GEAR-like ODE solver may be used.

However, in other circumstances, it is quite possible for transport to be intimately coupled with chemistry and vice versa. Kee and Miller [17] found that hydrogen which diffuses very readily in comparison with other chemical species negates the assumption that transport is essentially frozen in comparison to chemistry. Chang *et al.* [18] using the method of lines technique in modeling the photochemistry of the upper atmosphere found that ozone photochemistry was tightly coupled to its transport. Consequently, it was more efficient not to use any operator splitting, but to solve for both the chemistry and transport simultaneously.

Recently Kooker [19] employed the BI scheme to model a propagating O_2–O_3 flame in a confined vessel. He was able to freeze transport, while integrating the chemistry. This procedure worked well for O_2–O_3 flames but Kee and Miller [17] found that freezing the transport did not work well if hydrogen was present. For this reason, Kooker [19] found that the noniterative BI scheme was sufficient. Because of confinement, the acoustic waves interacted with the flame front to accelerate it. Although the BI scheme was stable for a time step greater than the CFL restriction, the results of such a calculation gave poor agreement with the experimental flame trajectory. However, when Δt was reduced to the burnt gas CFL limit to follow these acoustic interactions, the results were in excellent agreement with the experiment.

In contrast, Lund [20] investigated both ignition and flame propagation. Using a 1-D implicit Lagrangian scheme with an explicit Eulerian remapping and dynamic rezoning, he modeled an O_2–O_3 flame with 3 species and 3 reactions, and a CH_4–O_2 flame at 0.05 atm with 15 species and 45 reactions. Both flames were modeled from ignition to steady state flame propagation. During the ignition stages, he used time

steps ranging from 6×10^{-7} to 10^{-6} sec. As the flame approached steady state, he used time steps on the order of 3×10^{-5} sec. For the O_2–O_3 flame, he used time steps ranging from 10^{-9} sec to account for the initial fast kinetic rates to come to equilibrium, and later used time steps much greater than the CFL restriction. In contrast to Kooker [19], Dywer *et al.* [21], and Otey [22], Lund used a Newton–Raphson scheme to iterate the advanced time solutions to convergence. Using the same strategy as the stiff ODE solvers, he attempted to use the old Jacobian decomposition as long as possible in order to minimize expensive matrix decompositions. He found that a considerable saving of time could be realized if the matrix routines were written in assembly language rather than in Fortran.

In countering the reluctance of many to even consider implicit techniques because the inversion of large matrices is involved, Lund has shown, at least for the problems he has considered, that the time spent in calculating the physics is comparable to the time spent in the assembly language matrix decomposition routines.

Bathe and Cimento [23] considered Newton-like iteration schemes to solve the trapezoidal implicit response finite element equations of structural mechanics. They argued that one iteration step schemes resulting from the linearization of a configuration at the time t are only accurate provided the load increments or time steps are sufficiently small. Because of cost considerations, one endeavors to use as large a time step or load step as possible. Errors resulting from linearization about the time t may become quite large, and the error accumulation can lead to gross errors or instability. Hence, iteration about the new time solution, they concluded, is desirable at all load and time steps.

From this brief literature survey, a progression of thought can be found treating gas dynamics with combustion. Namely, the conservation equations are strongly coupled, an implicit formulation is highly desirable, and iteration of the implicit finite difference equations is necessary. The most robust of the schemes is the one developed by Lund [20] who used a Lagrangian–Eulerian implicit scheme with Newton–Raphson iteration. Lund has shown that the time spent in matrix algebra is comparable to the time spent calculating the physics and chemistry, at least in one-dimension.

This paper will use the block implicit-ADI scheme as a starting point for multidimensional combusting flows and introduce a modified type of Newton–Raphson iteration which is more powerful than the usual Newton–Raphson scheme and apply it to one- and two-dimensional combusting flows prior to, during, and after ignition.

III. The Finite Difference Scheme

The numerical modeling of chemically reacting fluid flow problems is complicated by such factors as: (1) the diversity of the time constants, and (2) the possible numerical instabilities generated by the numerical truncation errors. The full set of equations is given in the Appendixes. In abbreviated form, the set of L governing

PDEs, Ψ, in terms of the dependent variables in conservative form, Φ, has the structure

$$\begin{aligned} \Psi(\Phi) &= \partial\Phi/\partial t + H(\Phi), \\ H(\Phi) &= O_x(\Phi) + O_y(\Phi) + S(\Phi), \end{aligned} \tag{1}$$

where Ψ is the vector representative of the residuals, and where S is the vector representation of all the source terms and the cross derivative terms of the viscous dissipation; O_x and O_y are operators representing pressure gradients, convective flux divergences, and physical diffusion along the x and y axes, respectively, having the forms

$$O_x = \partial F/\partial x - \partial/\partial x[\sigma_x \partial(JX)/\partial x], \tag{2}$$

$$O_y = \partial G/\partial y - \partial/\partial y[\sigma_y \partial(JY)/\partial y], \tag{3}$$

F and G are column vectors representing fluxes in conservative form in the x and y directions, and $\partial(JX)/\partial x$ and $\partial(JY)/\partial y$ and σ_x and σ_y are the respective diffusive fluxes and coefficients along the x and y axes.

The solution is discretized by grid points having spacings, Δx and Δy, in the x and y directions, respectively, and an arbitrary time step, Δt. The subscripts i, j and the superscript n refer to the grid points, x_i, y_j, and t^n. Thus ϕ_{ij}^n denotes $\phi(x_i, y_j, t^n)$.

In this paper, a trapezoidal time marching scheme of maximum order 2 was used:

$$\Psi(\Phi_{ij}) = [\Phi_{ij}^{n+1} - \Phi_{ij}^n] + \Delta t\{\Theta H^1(\Phi_{ij}^{n+1}) + (1-\Theta) H^1(\Phi_{ij}^n)\} = 0$$

and

$$H' = O'_x + O'_y + S, \tag{4}$$

where Θ is a parameter which varies between zero and one, $0 \leqslant \Theta \leqslant 1$. O'_x and O'_y are selective finite difference operators which give rise to a three-point spatial differencing approximation for the physical diffusion and the pressure gradient terms. When O'_x and O'_y operate on the convective portion of the fluxes, F and G, respectively, the following donor-cell type scheme was used [2]:

$$\begin{aligned} O'_x(F_x) = (1/2\,\Delta x)[(F_{i+1,j} - F_{i-1,j}) - \{\varepsilon_+(F_{i+1,j} - F_{i,j}) \\ - \varepsilon_-(F_{i,j} - F_{i-1,j})\}], \qquad \{F = \rho u, \rho u^2, \text{etc.}\}, \end{aligned} \tag{5}$$

where the terms in brackets represents the upwind differencing contributions and are akin to a stabilizing numerical diffusion, and where

$$\begin{aligned} \varepsilon_\pm &= (\Delta t/\Delta x)(u_{i\pm1,j} + u_{i,j})/2 \qquad \text{if} \quad F \text{ refers to the convective term} \\ &= 0 \qquad\qquad\qquad\qquad\quad \text{if} \quad F \text{ refers to the pressure term.} \end{aligned} \tag{6}$$

If all the L finite difference equations for $\Theta \geqslant \frac{1}{2}$ together with the end point boundary conditions are solved simultaneously, one recognizes a block tridiagonal structure of the finite difference equations.

In this paper, a nonstaggered mesh system was used in contrast to the staggered mesh systems of the ICE codes. Since either system requires linear interpolation for flux formulations, a staggered mesh system does not appear to have any distinct advantage except at wall boundaries.

In a premixed flame, the characteristic length across the flame front is quite short. Consequently, very fine spatial resolution is required for accurate modeling. Another consideration is the speed at which a flame front travels relative to sonic disturbances in deflagrations. Computationally, it is desirable to use time steps comparabe to the flame front motion rather than sonic disturbances if sonic disturbances are unimportant. But there exist situations in which acoustic waves interact with the flame front, cf. [19, 24, 25]. This paper is, however, limited to flows for which such interactions are unimportant.

In summary, the important timescales of interest in unconfined highly transient chemically reacting fluid flow problems are the times: (a) to traverse the smallest computational cell by convection, (b) the fastest characteristic diffusion time across a diffusion length, l, (c) the adiabatic self-heating time of chemical enthalpy production (and (d) the characteristic sonic time across a cell for significant pressure gradients). These timescales assume all the processes are decoupled which is not true, in general. A lower bound on the timescale, assuming decoupling, is given by

$$\Delta t \leqslant \min \left[\frac{\min(\Delta x, \Delta y)}{\sqrt{\{u^2 + v^2\}_{\max}}}, l^2/\sigma_{\max}, \frac{p}{\{(\gamma - 1)\dot{q}_{\text{chem}}\}_{\max}}, \left\{ \frac{\rho u}{\nabla(p + \rho u^2)_{\max x,y}} \right\} \right], \tag{7}$$

where $\gamma = c_p/c_v$ is the effective physical diffusion length, $l = |\Phi/\nabla\Phi|$, σ is the corresponding physical diffusion coefficient, and u and v are the convective velocities in the x and y directions, respectively. The last term in Eq. (7) attempts to sense any significant pressure gradients (in the limit of no flow and no pressure gradient, the timescale tends to infinity) and approximates the CFL condition. This method was used successfully in [25], but has not been tested extensively.

Associated with any finite difference scheme are the problems of truncation errors. Sometimes, the numerical truncation errors in the presence of large gradients behave like a large positive numerical diffusion error which may be orders of magnitude greater than the physical diffusion. The cell Reynolds number problem discussed by Roache [2] or the negative destabilizing diffusion errors discussed by Rivard *et al.* [4] may become large enough to drive a numerical scheme unstable. If the numerical diffusion becomes too large, then either the spatial or temporal mesh or both should be refined. The literature contains a variety of recipes for treating the undesirable effects of numerical diffusion, and one such review has been recently presented by McDonald [26].

The approach used in the calculations to be presented later follows the ideas of Rivard *et al.* [4] and Chien [27] who added terms to the FDEs in such a manner that the modified equations have minimized the overall truncation errors. There are two sources of numerical diffusion: the spatial truncation errors, ERR_s, which arise from the finite difference treatment of the convective terms, and the temporal truncation errors, ERR_t, arising from the trapezoidal time marching scheme. If the donor cell scheme was not used,

$$\mathrm{ERR}_s = (\Delta x/2)(uA\Phi_x)_x + (\Delta y/2)(vB\Phi_y)_y; \qquad A = \partial F/\partial \Phi,\ B = \partial G/\partial \Phi. \tag{8}$$

However, this velocity dependent error is accounted for by the donor cell differencing scheme, cf. Eq. (5).

$$\mathrm{ERR}_t = (2\Theta - 1)[(A^2\Phi_x)_x + (B^2\Phi_y)_y + (AB\Phi_y)_x + (BA\Phi_x)_y](\Delta t/2) + \cdots. \tag{9}$$

Note that when $\Theta = \frac{1}{2}$ which corresponds to the second-order accurate scheme, the lowest order terms of ERR_t vanish. McDonald [26] recommends that the diffusive cross derivative terms be treated explicitly with no serious loss of stability, and such terms in this paper will be lumped into $S(\phi_{ij}^n)$ for convenience. To ensure against the possibility of truncation error diffusion errors arising from the higher-order terms, a small amount of residual positive numerical diffusion was retained. This was done by adding a small term, ν, to the time splitting parameter, Θ, so that

$$\Theta = \tfrac{1}{2} + \nu, \tag{10}$$

where $\nu = 0.02 * D$ and D is the smallest diffusion coefficient expressed in dimensionless form. Note that by retaining a small amount of positive numerical diffusion even the conservation of mass equation is cast into parabolic form.

The module just described for treating numerical diffusion can be readily replaced by the flux corrected transport method of Boris and Book [28]; the tensor viscosity method of Ramshaw and Dukowics [6]; or the fourth-order filtering method of Beam and Warming [13]. However, the best remedy for the truncation error problem is adequate grid resolution when needed. Dwyer *et al.* [21] presented an adaptive coordinate transformation which automatically adjusts itself to a dependent variable gradient as the system evolves to ensure adequate spatial resolution. Concurrently, Lund [20] developed a dynamic rezoning technique which gives very fine spatial resolution in regions of steep gradients, but also gives gradually coarser resolution away from such regions.

IV. An Iterative Block Implicit-ADI Algorithm

It was the author's experience that the noniterative BI-ADI scheme was inadequate in treating a wide range of combustion problems unless prohibitively small time steps were used. In this section, the nonlinear truncation errors which could be

destabilizing are examined in the advanced time solutions. In a manner similar to the Gear [29, 30] schemes, such errors are kept under control thus rendering the modified BI-ADI scheme more robust. The remainder of this section will discuss the efficiency of various iteration schemes which is essential to the overall modified BI-ADI scheme.

Carver [31] attributes the vitality of the stiff ODE algorithms to the implicit finite difference formulation, the use of Newton-like iteration schemes to solve the nonlinear FDEs, and the step length control based on the conditioning of the Jacobian, i.e., the rate of convergence. Recently, Beam and Warming [32–34] discussed the importance of developing the methods and analyses adopted from the ODE methods that can be directly applied in the development of efficient stable PDE algorithms.

The basic motivation for solving ODEs and PDEs by an implicit time marching scheme is to circumvent the explicit stability requirement which may be orders of magnitude more restrictive than physical accuracy requirements. Because larger time steps are permitted in implicit schemes, the nonlinear truncation errors may become very large. Just as the stiff ODE solvers introduce a variation of the Newton–Raphson (NR) scheme to bring the nonlinear truncation errors under control, so will the NR scheme be introduced to the BI-ADI scheme rendering it suitable to a wider class of problems.

The basic noniterative BI-ADI technique of Briley and McDonald [12] and Beam and Warming [13] replaces the PDEs by an implicit ($\Theta \geqslant \frac{1}{2}$) trapezoidal time marching scheme whereby all the terms involving nonlinearities at the advanced time steps are linearized by a Taylor expansion at the known time level, and spatial differencing is introduced. To solve the multidimensional problem, an ADI scheme, using the full time step rather than fractional time steps, is introduced which successively approximates the true time advanced solutions by successively including more spatial transport terms at the advanced time step.

The system of PDEs to be solved has the structure

$$\Psi(\Phi) = \frac{\partial \Phi}{\partial t} + H(\Phi) = 0 \tag{1}$$

which is approximated by the trapezoidal time marching scheme:

$$\Psi(\Phi^{n+1}) = \Phi^{n+1} - \Phi^n + \Delta t\{\Theta H'(\Phi^{n+1}) + (1 - \Theta) H'(\Phi^n)\} = 0, \tag{4}$$

where

$$H'(\Phi) = H(\Phi) - (2\Theta + \kappa - 1) * [(A^2\Phi_x)_x + (B^2\Phi_y)_y + (AB\Phi_y)_x + (BA\Phi_x)_y](\Delta t/2) \tag{11}$$

and κ is a parameter which counteracts the negative destabilizing numerical diffusion and reduces excessive positive diffusion, cf. Rivard *et al.* [4, 5].

In the BI scheme, the problem is linearized by expanding H'^{n+1} about Φ^n, and by replacing

$$\Delta t \left(\frac{\partial \Phi}{\partial t}\right) \simeq \delta\Phi^{n+1}(1), \tag{12}$$

where

$$\delta\Phi^{n+1}(1) = \Phi^{n+1}(1) - \Phi^n. \tag{13}$$

These approximations result in the following form of the residual:

$$\Psi^{n+1} = J\,\delta\Phi^{n-1}(1) + \Delta t(H'^n) + \underline{\left(\frac{\Delta t}{2}\,\delta\Phi^T \frac{\partial^2 H'}{\partial \Phi^2}\,\delta\Phi\right)} + \cdots \simeq 0, \tag{14}$$

where

$$J = I + \Delta t\,\Theta \frac{\partial H'}{\partial \Phi}, \tag{15}$$

I is the identity matrix, and the underlined terms are the higher-order nonlinear truncation errors, corresponding in the BI scheme to the higher-order temperal truncation errors, $\mathrm{ERR}_{\mathrm{nl}}$.

Neglecting the nonlinear truncation errors, the BI scheme yields the correction

$$\delta\Phi^{n-1}(1) = -J^{-1}(\Delta t\, H'^n) \tag{16}$$

so that

$$\Phi^{n+1}(1) = \Phi^n + \delta\Phi(1)^{n+1}. \tag{17}$$

For the noniterative scheme to be accurate, Ψ must be linear about Φ^n, and Eq. (14) is an accurate approximation to Eq. (4). Ψ is said to be sufficiently linear, if the Euclidean norm of Ψ, given by Eq. (4) using the noniterative value of $\Phi^{n+1}(1)$ from Eq. (17), is less than some tolerance, i.e.,

$$\|\Psi(\Phi(1))\|_2 < \varepsilon = 10^{-6}. \tag{18}$$

If this test fails, then Ψ is said to be nonlinear. Equation (16) for obtaining $\delta\Phi^{n+1}(1)$ requires a formidable matrix inversion effort in two or three spatial dimensions. However, $\delta\Phi^{n+1}(1)$ may be obtained by a series of simpler block tridiagonal problems which approximates Eq. (16) by a consistent sequence of simpler problems.

First, solve for an approximate $\delta\Phi^*$ during the x sweep in which the transport terms are totally explicit along the y coordinate, but partially implicit along the x coordinate.

$$J^*\,\delta\Phi^* = -\Delta t\, H'^n, \tag{19}$$

where

$$J^* = I + \Delta t\, \Theta \left\{ \frac{\partial O_x}{\partial \Phi} + \frac{\partial S}{\partial \Phi} \right\}, \tag{20}$$

and

$$\Phi^* = \Phi^n + \delta\Phi^*, \tag{21}$$

Using the updated Φ^*, perform the y sweep solving

$$J^{**}\,\delta\Phi^{**} = -\Delta t \left\{ H'^n + \Theta \frac{\partial O_x}{\partial \Phi}\,\delta\Phi^* \right\}, \qquad J^{**} = I + \Delta t\, \Theta \left[\frac{\partial O_y}{\partial \Phi} + \frac{\partial S}{\partial \Phi} \right] \tag{22}$$

which is consistent with Eq. (14) yielding

$$\Phi^{n+1} = \Phi^{**} = \Phi^* + \delta\Phi^{**}. \tag{23}$$

If $\Theta = \frac{1}{2}$, a second-order accurate scheme is used. A natural extension of the BI-ADI scheme is the introduction of a Newton-like iteration scheme which controls the nonlinear truncation errors by both time step control and contractive norm reduction, but not solely by time step control. The iterative extension of the noniterative BI-ADI scheme is justified if the total number of arithmetical operations with iterations using a larger time step is less than that of the noniterative scheme using a smaller time step with many time cycles.

In contrast to the BI scheme, the nonlinear terms in this paper are linearized about the current iterate, $\Phi^{n+1}(k)$, of the advanced time solution vector,

$$H'[\Phi(k+1)] = H'[\Phi^{n+1}(k)] + \left(\frac{\partial H'}{\partial \phi} \right) \delta\Phi(k+1) + \frac{1}{2}\,\delta\Phi^T(k+1) \left(\frac{\partial^2 H'}{\partial \phi^2} \right) \delta\Phi(k+1) + \cdots \tag{24}$$

so that

$$\Psi(\Phi^{n+1}(k+1)) \simeq \Psi(\Phi^{n+1}(k)) + \left\{ I + \Delta t\, \Theta \left(\frac{\partial H'}{\partial \Phi} \right) + \underline{\frac{\Delta t}{2}\, \Theta\, \delta\Phi^T(k+1) \left(\frac{\partial^2 H'}{\partial \Phi^2} \right)} \right\} \delta\Phi(k+1) + \cdots \simeq 0, \tag{25}$$

where

$$\Psi(\phi^{n+1}(k)) \simeq \Phi^{n+1}(k) - \Phi^n + \Delta t\{\Theta H'[\Phi^{n+1}(k)] + (1-\Theta)\, H'[\Phi^n]\}, \tag{26}$$

$$\delta\Phi(k+1) = \Phi^{n+1}(k+1) - \Phi^{n+1}(k). \tag{27}$$

Note that the iterative extension involves a consistent sequence of approximations to the original residual vector Ψ, cf. Eq. (2), including both transport and source terms at the advanced time level.

The iteration scheme can be initialized by choosing the first iterate at the advanced time to be the old solution vector, i.e.,

$$\Phi^{n+1}(k=0) = \Phi^n. \tag{28}$$

Other initialization schemes are also possible. If the iterative scheme is convergent, successive approximations will contract both the norms of the residuals and the correction vectors, i.e.,

$$\| \Psi(\phi^{n+1}(k+1))\| < \| \Psi(\Phi^n(k))\|, \tag{29}$$

$$\| \delta\phi(k+1)\| < \| \delta\Phi(k)\| \tag{30}$$

reducing the nonlinear contributions to a point where Ψ is linear about $\Phi^{n+1}(k+1)$, and

[redacted]

Note that if Δt is chosen small enough, and if convergence is obtained in one iteration, the iterative BI scheme is identical to the noniterative BI scheme.

The ADI scheme used here is similar to the BI scheme, except the intermediate solutions are iterated to convergence for each sweep. The standard Newton–Raphson procedure neglects the nonlinear higher-order corrections from the Hessian.

For the x-sweep of the ADI scheme, set $\Phi^*(0) = \Phi^n$ and solve

$$J^*(k)\, \delta\Phi^*(k+1) = -\Psi^*(k), \tag{33}$$

where

$$J^*(k) = I + \Delta t\, \Theta \left\{ \frac{\partial O_x}{\partial \Phi} (\Phi^*(k)) + \frac{\partial S}{\partial \Phi} (\Phi^*(k)) \right\}, \tag{34}$$

$$\begin{aligned} \Psi^*(k) = \Phi^*(k) - \Phi^n + \Delta t \{ & \Theta \{ O_x(\Phi^*(k)) + S(\Phi^*(k)) \} \\ & + (1-\Theta)\{ O_x(\Phi^n) + S(\Phi^n) + O_y(\Phi^n) \} \} \end{aligned} \tag{35}$$

and,

$$\Phi^*(k+1) = \Phi^*(k) + \delta\Phi^*(k+1). \tag{36}$$

The iteration continues until

$$\| \Psi^*(k+1)\| < \varepsilon, \tag{37}$$

$$\| \delta\Phi^*(k+1)\| < \eta, \tag{38}$$

and

$$\Phi^*(k+1) \to \Phi^*. \tag{39}$$

For the y sweep, set $\Phi^{**}(0) = \Phi^*$, and solve

$$J^{**}(k)\,\delta\Phi^{**}(k+1) = -\Psi^{**}(k), \tag{40}$$

where

$$J^{**}(k) = I + \Delta t\,\Theta\left\{\frac{\partial O_y}{\partial \Phi}(\Phi^{**}(k)) + \frac{\partial S}{\partial \Phi}(\Phi^{**}(k))\right\}, \tag{41}$$

$$\Psi^{**}(k) = \Phi^{**}(k) - \Phi^n + \Delta t\,\Theta\{O_y(\Phi^{**}(k)) + S(\Phi^{**}(k)) + O_x(\Phi^*)\} + (1-\Theta)\,\Delta t\{O_x(\Phi^n) + O_y(\Phi^n) + S(\Phi^n)\}, \tag{42}$$

$$\Phi^{**}(k+1) = \Phi^{**}(k) + \delta\Phi^{**}(k+1). \tag{43}$$

The iteration continues until

$$\|\Psi^{**}(k+1)\| < \varepsilon, \tag{44}$$

$$\|\delta\Phi^{**}(k+1)\| < \eta, \tag{45}$$

and

$$\Phi^{**}(k+1) \to \Phi^{**} = \Phi^{n+1}. \tag{46}$$

Newton's method is an iterative scheme in which each step involves the solution of a linear problem. When it converges, there is a successive norm reduction of the correction which proceeds at a quadratic rate, i.e.,

$$\|\delta\Phi(k+1)\| \leqslant \text{const}\,\|\delta\Phi(k)\|^2. \tag{47}$$

Consequently, in a convergent condition, the nonlinear truncation errors will be reduced more efficiently by both time step reduction and iteration than solely time step reduction, cf. Briley and McDonald [35].

Briley and McDonald [35] pointed out that an iterative BI scheme is justified if the nonlinear truncation errors, ERR_{nl}, are greater than the temporal truncation errors. Reducing Δt reduces ERR_t and ERR_{nl} simultaneously whereas successive iterations rapidly reduce ERR_{nl}, while leaving ERR_t unaffected. However, iterations are more efficient than reducing Δt if ERR_{nl} is greater than ERR_t.

The efficiency of the IBI scheme depends upon the conditioning of the Jacobian. The system $J\,\delta\Phi = -\Psi$ is said to be ill conditioned if small errors in J or Ψ yield large errors in $\delta\Phi$. Following Goult *et al.* [36], a useful bound on the convergence of the correction vector is given by

$$\frac{\|\delta\Phi(k+1) - \delta\Phi(k)\|}{\|\delta\Phi(k)\|} \leqslant \frac{K}{1 - K\,\|\delta J\|/\|J\|}\left\{\frac{\|\delta J\|}{\|J\|} + \frac{\|\delta\Psi\|}{\|\Psi\|}\right\}, \tag{48}$$

where

$$\delta J = \frac{\Delta t\, \Theta}{2} \delta \Phi^T(k) \frac{\partial^2 H'}{\partial \Phi^2}, \tag{49}$$

$$\delta \Psi = \Psi(k+1) - \Psi(k) \tag{50}$$

and

$$K = \|J^{-1}\| \cdot \|J\|, \tag{51}$$

is the condition number. The smaller the condition number, the smaller will be the errors in $\delta\Phi$ as a result of inaccuracies in J or Ψ.

Following Ortega and Rheinboldt [37], a matrix which is diagonally dominant is invertible. A well conditioned matrix has the ratio of absolute value of its largest to smallest eigenvalue near unity and dampens errors in Ψ or J rapidly, so that

$$K\,\|\delta J\|/\|J\| \ll 1. \tag{52}$$

Furthermore, the matrix which arises from the Crank–Nicholson finite difference formulation of the parabolic heat conduction PDE is an example [37] of a well conditioned, diagonally dominant, positive definite matrix. Likewise, it can be shown that the hyperbolic portion of the conservation equations gives rise to well conditioned matrices if the convective terms are differenced implicitly ($\Theta \geqslant \frac{1}{2}$) and if the time step is within the convective limit. When a purely transport PDE involving convection and physical diffusion is differenced implicitly, it gives rise to a well conditioned diagonally dominant matrix. The effect of the destabilizing numerical truncation error diffusion terms is to shift a well conditioned matrix toward ill conditioning. Such errors must be kept within bounds by proper differencing techniques and adequate gridding.

Because the NR scheme involves a system of linear equations at each iterative step, the conditioning of the Jacobian matrix is just one important aspect. Convergence to a unique fixed point solution, Φ^{n+1}, is guaranteed by the Kantorovich theorem [37], as follows. If there exist upper bounds for the following quantities,

$$\begin{aligned} &\text{(a)} \quad \|J(0)^{-1}\| = \|(I + \Delta t\, \Theta(\partial H'/\partial \Phi)_0)^{-1}\| \leqslant \alpha, \\ &\text{(b)} \quad \|\partial^2 \Psi/\partial \Phi^2\| = \Delta t\, \Theta\, \|\partial^2 H'/\partial \Phi^2\| \leqslant \omega, \\ &\text{(c)} \quad \|\delta \Phi(1)\| = \|\Phi^{n+1}(1) - \Phi^n(0)\| \leqslant \beta \end{aligned} \tag{53}$$

and if

$$h = \alpha\omega\beta < \tfrac{1}{2}, \tag{54}$$

then the rate of convergence to a unique fixed point Φ^{n+1} proceeds quadratically

$$\|\Phi^{n+1} - \Phi^{n+1}(k+1)\| \leqslant \frac{(2h)^{2^{k-1}}}{2^{k-1}} \|\delta \Phi(1)\|. \tag{55}$$

In contrast, the MSS iteration scheme which is an "explicit iteration" scheme, as applied in the RICE [4, 5] and APACHE [6] schemes

$$\Phi^{n+1}(k+1) = -\Delta t\, \Theta H'(\Phi^{n+1}(k)) + \Phi^n - (1-\Theta)\,\Delta t\, H'^n \tag{56}$$

converges linearly to a unique Φ^{n+1} provided

$$\Delta t\, \Theta \left\| \frac{\partial H'}{\partial \Phi} \right\| < 1. \tag{57}$$

The convergence criterion for the MSS iteration scheme may have restrictive time step limitations, whereas the time step restriction is critical in the NR scheme only if the Jacobian becomes ill conditioned. In the transport dominated regime, the Jacobian is well conditioned according to linear theory. Also in this regime, one also expects the nonlinear contributions to be small making the norm of the Hessian small. However, with Arrhenius kinetics, this term may be quite large. Finally, the third term, the initial error in the correction vector, is expected to be quite small during a transport dominated flow, but could be quite large, for a given time step, during an ignition process. During ignition, the initial guess, $\Phi^{n+1}(0) = \Phi^n$, may be a poor starting point for the iteration process, and other initialization procedures may be necessary.

The radius of convergence of the MSS and NR iteration schemes are given by

$$r_{\mathrm{MSS}} = \frac{1}{1 - \Delta t\, \Theta \|\partial H/\partial \Phi\|} \|\Phi^{n+1}(1) - \Phi^{n+1}(0)\| \tag{58}$$

for the MSS scheme and for the NR scheme,

$$r_{\mathrm{NR}} = (1 - \sqrt{1-2h})\, \frac{\|\delta\Phi(1)\|}{h}, \tag{59}$$

where h is given by Eq. (54).

The radius of convergence of the NR scheme is at least twice that of the MSS scheme. Only when the initial guess is quite close to the fixed point solution will the MSS scheme be more efficient than the NR scheme. To illustrate this point, consider the implicit-ADI shallow water calculations of Gustafsson [38]. For a time step four times greater than the CFL condition, NR schemes converged whereas the MSS scheme diverged. However, if the time step was less than four times the CFL condition and the solution was smooth, MSS proved to be more efficient than NR schemes from an operational count viewpoint.

If one starts an iteration scheme within the sphere of convergence of the Newton–Raphson (NR) scheme, the NR scheme will converge quadratically; if not, it will diverge disasterously. A number of modifications of the basic NR scheme have been developed that try to provide reliable convergence even when a good estimate of the solution is not available. The scheme used in this paper follows the hybrid method

of Powell [39] which biases the iteration corrections toward the steepest descent (SD) direction if the full NR corrections are too large or are in the wrong direction. This scheme is particularly attractive since the information utilized by the NR scheme can also be readily used by the SD scheme with comparatively few extra arithmetical operations.

The NR correction vector is given in terms of the inverse of the Jacobian:

$$\delta\Phi_{\mathrm{NR}} = -[J^k]^{-1}\, \Psi(\Phi^k), \tag{60}$$

whereas the SD correction vector is given in terms of the transpose of the Jacobian:

$$\delta\Phi_{\mathrm{SD}} = -[J^k]^T\, \Psi(\Phi). \tag{61}$$

The correction vector recommended by Powell is a linear combination of the damped Newton–Raphson and steepest descent correction vectors:

$$\delta\Phi = \zeta\, \delta\Phi_{\mathrm{NR}} + (1-\zeta)\mu\, \delta\Phi_{\mathrm{SD}}, \tag{62}$$

where ζ and μ are constants which are dynamically determined in Powell's algorithm to minimize the residuals, Ψ.

In the LSODE package developed by Hindmarsh and Byrne [40], several improvements were made to the older GEAR package such as dynamic variable step size criterion and banded matrix storage and manipulation. Depending upon the problem, in some cases the same Jacobian can be used for about five step lengths with one or two iterations per time step. In more extreme cases, it was found necessary, not only to update the Jacobian every iteration of the time marching cycle, but also to adjust the time step during periods of highly nonlinear, transient processes.

The Jacobian and its decomposition may be held fixed provided the rate of convergence is satisfactory during a particular ADI sweep. However, in a two- or three-dimensional problem, all the old Jacobians and their decompositions from each ADI sweep would, most likely, not be able to be stored in fast core memory. Depending upon the computer available, it may be possible to store the old Jacobians and their decomposition on disk file. Such a strategy would be efficient if the I/O time of disk reads and writes were at least comparable to the fast core arithmetical operations.

Because of the various classifications of difficulty and complexity possible in combusting gasdynamic systems, and the unequality of computer systems which are available, this paper advocates flexibility in replacing various modules by those which could be best suited for a particular problem. One must decide whether one can sacrifice fast core computer memory for a more efficient module, or settle for a less efficient module which uses far less computer memory. One such module that is worthwhile considering is the approximate updating schemes of the Jacobian and its decompositions during periods of rapid, highly nonlinear transients which have been

discussed by Powell [39] and Broyden [41]. The strategies developed in other research areas, such as electrical engineering, for solving large systems of nonlinear equations might prove to be very useful for combusting fluid dynamics.

V. Time Step Control in Stiff ODE and PDE Solvers

As Carver [31] has stated, the robust nature of stiff ODE solvers is partly due to dynamic time step control. This section will discuss the problem of dealing with a which is unconditionally stable in a transport dominated regime can be driven unstable in a highly exothermic combustion regime (ignition) unless proper time step control is exercised. Because it is possible in combustion phenomena to find situations in between either ends of the spectrum from the familiar aerospace transport dominated flows to pure Arrhenius kinetics, a PDE solver must be robust enough to handle any range of situations.

In the aerospace applications of Warming and Beam [42], the advantages of the delta formulation or the Douglas–Gunn [14] ADI scheme are (in the absence of source terms): the steady state is independent of Δt; easy application of the boundary conditions; and general time differencing with a trivial change of parameters. According to linear theory, the Douglas–Gunn ADI scheme is unconditionally stable. Briley and MacDonald [35] argue that with the use of the BI-ADI scheme that steady state, if it exists, can be achieved quickly by cycling through large and small time steps if accurate transient solutions are unnecessary. In contrast, one of the serious defects of the fractional time step ADI scheme is that its steady state solution is time step dependent.

A rigorous analysis of the governing set of PDEs which occur in combusting gasdynamic systems will not be attempted. However, the examination of a much simpler problem analogous to the real problem is useful. Consider a 1-D gasdynamic combustion problem in which all physical diffusion terms are neglected. Since the PDEs are in conservative form, the convective portion can be replaced by

$$A = \partial F/\partial \Phi; \tag{63}$$

cf. [1, 2]. Assume the convective flow is positive, and use upwind spatial differencing. In the time interval, Δt, assume that the source terms, $S(\Phi)$, can be linearly approximated by $S(\Phi) = -\Lambda\Phi$, where Λ is a diagonal matrix having eigenvalues, (λ_i), which may assume any value in the complex plane. The governing set of PDEs is now replaced by the following inhomogeneous ODE at the location x_i:

$$d\Phi_i/dt = \Lambda'\Phi_i + (A/\Delta x)\,\Phi_{i-1}, \tag{64}$$

where $\Lambda' = \Lambda - A/\Delta x$. In the time interval, Δt, assume the inhomogeneous term and the A matrix are approximately constant. Equation (64) then has an exact solution of the form

$$\Phi_i^{n+1} = \Phi_i^n \exp(\lambda_i' t^n) + (A/(\Delta x\,\Lambda'))\,\Phi_{i-1}. \tag{65}$$

The general linear multistep method, cf. Seinfeld *et al.* [43], has the form

$$\Phi^{n+1} = \sum_{i=1}^{k} a_i \Phi^{n+1-i} + (\Delta t) \sum_{i=0}^{k} b_i \Phi^{n+1-i}. \tag{66}$$

The numerical solution is given in terms of characteristic roots, f,

$$f^k - \sum_{i=1}^{k} a_i f^{k-i} - (\Delta t\, \lambda') \sum_{i=0}^{k} b_i f^{k-i} = 0. \tag{67}$$

One of the characteristic roots which approximates the Taylor expansion of the true homogeneous solution, $f = \exp(\Delta t\, \lambda')$, is denoted by f_1; the other roots are spurious. A linear multistep method is: (a) absolutely stable if every characteristic root is bounded by unity, $|f_i| \leqslant 1$ for all i; (b) relatively stable if $|f_i| \leqslant |f_1|$ for all $i \geqslant 2$.

It is interesting to note that if $\mathrm{Re}(\lambda_i') < 0$, any integration rule is inherently stable for all values of $\Delta t > 0$; the exact homogeneous solution decreases exponentially with t^n. However, if $\mathrm{Re}(\lambda_i') > 0$, the exact solution grows with t^n; the important concern is the relative stability. Seinfeld *et al.* point out that this will be a valid solution as long as no component of the numerical solution increases faster than the one corresponding to the principal root. They also point out that even if $\mathrm{Re}(\lambda_i') < 0$, the absolutely stable regime, the trapezoidal rule is very inaccurate for very large, negative values of λ' because it tends to -1 rather than to 0 which would occur in the exact method. This problem of gross inaccuracy can be avoided by either a simple filtering procedure or using small step lengths in those initial phases when the stiff solutions are noneligible. Note that in the absence of source terms, the trapezoidal rule for Eq. (64) is unconditionally stable for $\Theta > \frac{1}{2}$, at least according to linear theory.

Boggs [44] has made a connection with the damped Newton–Raphson iteration scheme with the A-stable ODE integration schemes. The time marching scheme used to integrate the conservation equations may be viewed as an iteration process by which either a nonsteady or steady state solution evolves from an initial state with the time step parameter playing the role of a damping constant of the overall Newton–Raphson iteration process. If the damped NR scheme is viewed as a class of Davidenko differential equations, then the stability analysis of Dahlquist [45] used for A-stable ODE schemes can also be used in developing efficient, stable iteration schemes for nonlinear equations. Boggs [44] recommends that the damping factor or step length be chosen by considering the norm of the residuals and using a trapezoidal average of the old and updated NR correction vectors for increased stability. To minimize excessive updating of the Jacobian and its decomposition, he recommends the approximate updating procedure of Broyden [41]. From Boggs [44], one can infer that while NR iteration schemes correspond to A-stable ODE schemes, the MSS iteration scheme corresponds to an explicit one leg ODE scheme, with a similar restrictive region of stability and convergence.

Time step control is also necessary to ensure that the Jacobian is well conditioned.

Referring to Eq. (64), the trapezoidal time marching schemes give rises to a block bi-diagonal structure of the form

$$A'\Phi_{i-1}^{n+1} + B'\Phi_i^{n+1} = Z_i, \tag{68}$$

where $A' = -\Delta t\,\Theta A/\Delta x$, $B' = (I - \Theta\,\Delta t\,A')$, and $Z' = [\Phi_i^n + (1-\Theta)\,\Delta t\{A'\Phi_i^n + A/\Delta x\,\Phi_{i-1}^n\}]$. If every eigenvalue of A' is negative, the Jacobian is always well conditioned. If at least one eigenvalue is positive, then in order for the block bi-diagonal scheme to be decomposable, it is sufficient that $B' > 0$, i.e.,

$$\Delta t < 1/(\Theta\lambda_i'). \tag{69}$$

As this simplified system approaches steady state, the exothermic chemistry and the convective transport tend to balance, thereby permitting larger time steps. Concerning multidimensional problems, an eigenvalue analysis of the Jacobian would provide accurate information for choosing the optimum time step; however, such an analysis is impractical. The Jacobian of a system of nonlinear equations is well conditioned if it is positive definite, and preferably diagonally dominant. Heuristically, this property can be ensured if the diagonal elements satisfy

$$\min_i \left\{ I + \Delta t\,\Theta \frac{\partial H'}{\partial \Phi} \right\}_{ii} > 0 \tag{70}$$

which is similar to the restriction on Δt given by Eq. (69). However, the criterion used in this paper in determining whether the proper time step is chosen is that both the norms of the correction vector and the residuals be convergent, cf. Eqs. (31), (32), for each coordinate sweep of the Douglas–Gunn ADI scheme. If a time step is chosen to ensure that the Jacobian is well conditioned at each stage and if the correction vectors and residuals are convergent, then the Kantorovich theorem guarantees convergence to a unique solution, Φ^{n+1}. There are several areas of similarity and dissimilarity between the method of lines technique and this algorithm. The areas of similarity are: (a) the use of implicit time marching schemes, (b) the use of Newton-like iteration methods for solving the resulting set on nonlinear FDEs, and (c) the dynamic time step control based on the conditioning of the Jacobian. The areas of dissimilarity are: (a) the accuracy of the time marching scheme, i.e., trapezoidal of maximum order 2 versus various higher-order schemes, (b) matrix storage and decomposition, i.e., block tridiagonal versus banded, and (c) the frequency of updating the Jacobian and its decomposition during the time marching scheme. The last area of dissimilarity points out the difficulty in extending all the stiff ODE techniques to a multidimensional PDE problem when both the restrictions of computer memory and disk I/O operation efficiency become limiting factors.

In summary, this algorithm has incorporated not only the features of the Briley–McDonald and Beam–Warming BI-ADI scheme, but has also incorporated the features of the stiff ODE and nonlinear equation solver schemes. Because combusting gas dynamics are quite different from aerospace gas dynamics, careful

time step control is essential in regions of highly nonlinear exothermic Arrhenius chemistry to ensure that at least relative numerical stability is guaranteed. This algorithm is summarized in the Appendixes.

VI. Time Step Control and Multiple Solutions

Because multiple solutions are possible in systems of nonlinear PDEs, a major concern is whether the resulting solution is determined by the numerics rather than by the deterministic chemistry and physics. In this section, an analysis of this question which was not performed in a previous paper concerning coal dust flames is presented. Later in this section, a literature review will further examine the attainment of an incorrect multiple solution from the numerics rather than by the physics.

The calculations of Kansa and Perlee [46] on coal dust flames help illustrate the close coupling between transport and chemical enthalpy production that exists during periods of drastic timescale change. They assumed that a coal dust cloud could be approximated by an ensemble of independent microsystems which consisted of the coal particle and its surrounding gas volume. The coal particle was assumed to be a porous, permeable body which upon heating underwent Arrhenius pyrolytic decomposition producing char and combustible volatiles. In the gas subsystem, the following processes: molecular diffusion, convection, thermal conduction, and an irreversible second-order combustion reaction,

$$\text{Oxidant} + \text{volatiles} \rightarrow \text{Combustion products} \tag{71}$$

are included.

Given specific initial and boundary conditions, an interesting problem is to determine whether a characteristic steady state char burnout solution can be achieved within a specified time interval, cf. [46]. The determination of whether steady state is achieved within a characteristic time interval for plug flow coal dust flames depends strongly upon the transient pyrolysis process and volatile combustion process.

Physical argument and numerical experimentation [46] showed that a uniform mesh of 10 points more than adequately resolved the coal particle. Likewise, an exponentially stretching grid system of 20 points resolved the gas subsystem; the finest resolution of this grid network occurred near the coal particle. If the coal particle is smaller than 40 μm, it will absorb radiation volumetrically, cf. [46]. In addition, if the flame is of infinite extent compared to the coal particle and if the coal particle absorbs radiation volumetrically, then a one-dimensional model is sufficient.

Figure 1 illustrates an ignition phenomenon over a very short duration, i.e., a sharp spike in the fuel consumption rate. The solid line represents the log of the absolute value of $\dot{R}_{\text{fuel}}$. In this study, a 7.5-μm coal particle approaches a flame at 1800 K with an input velocity of 30 cm/sec. The coal particle, which is heated initially by radiation, begins to rapidly pyrolyze when the particle temperature exceeds 450 K. Because of the small length scales, molecular diffusion and convection rapidly mix the volatiles and oxidant within the gas system. Before 10.5 msec, up to point A, the

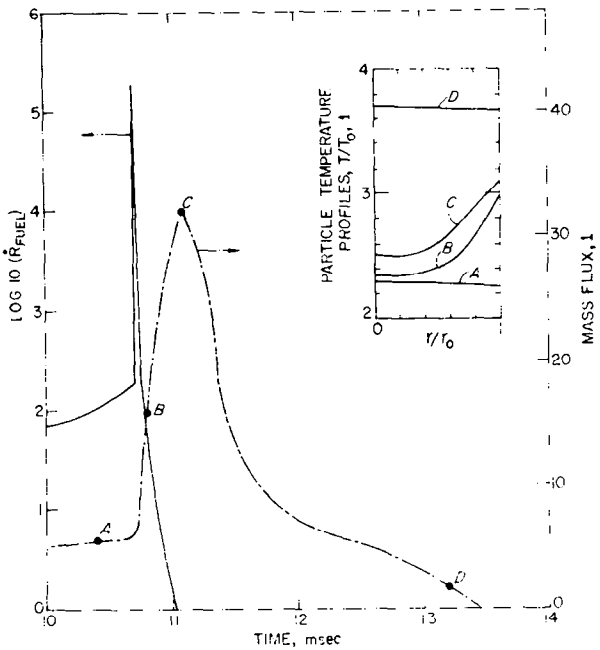

FIG. 1. The absolute value of the log of fuel consumption, the rate of coal pyrolysis and temperature profiles of a 490-mg l^{-1} coal dust flame around the time of gas phase ignition.

PDE solver used times steps on the order of 0.1 msec. However, immediately after point A, the gas temperature 3–5 particle radii from the surface exceeded 925 K, and, because of the Arrhenius kinetics, the gas mixture of volatile fuel and oxidant appeared to ignite homogeneously. Between points A and C, convergence could only be achieved by using time steps of 2-μsec duration. During the ignition period which is represented by the sharp spike, the gas temperature was around 2100 K, except near the coal particle.

Because a large thermal gradient was established at the particle surface during the ignition phase, the particle underwent accelerated heating and pyrolysis. The broken line in Fig. 1 represents the rate of solid pyrolysis. Because of the difference in thermal inertias between the gas and particle subsystem, the solid pyrolysis rate was a maximum at point C. After 11 msec, the ignition phase was terminated because the oxidant was completely consumed within the gas subsystem, slightly after point B. The coal particle continued to pyrolyze up to 13.5 msec, point D, after which the coal particle was completely converted to a char residue. As the pyrolysis reaction ran down, the time steps were increased to 0.25 msec. In addition, as the microsystem became progressively more inert, the Jacobian also varied progressively more slowly in time. The burning distance for fine coal particles has been measured to vary from 0.3 to 1.5 cm depending upon the dust concentration and input velocity. This model predicts that a 490 mg/liter dust cloud with an input velocity of 30 cm/sec will have

a burning length of 1.0 cm which is in excellent agreement with observation. This result indicates that although the chemistry is oversimplified, the physics is essentially correct for this type of coal dust flame.

The inset in Fig. 1 represents the particle temperature profiles at the times indicated by points A, B, C, and D. During periods of significant pyrolysis (due to heating by the burned gas phase), the coal particle temperature profiles are quite nonuniform, contrary to most opinions, because of the large amount of internal convective heat transport. Only when pyrolysis occurs very slowly can the temperature profile within the coal particle be assumed to be uniform.

Figure 2 shows the temperature and species mole fraction profiles in the gas subsystem, prior to, during, and after the gas phase ignition. Before ignition ($t = 10.673$ msec), the temperature, oxidant, and fuel molefraction profiles were

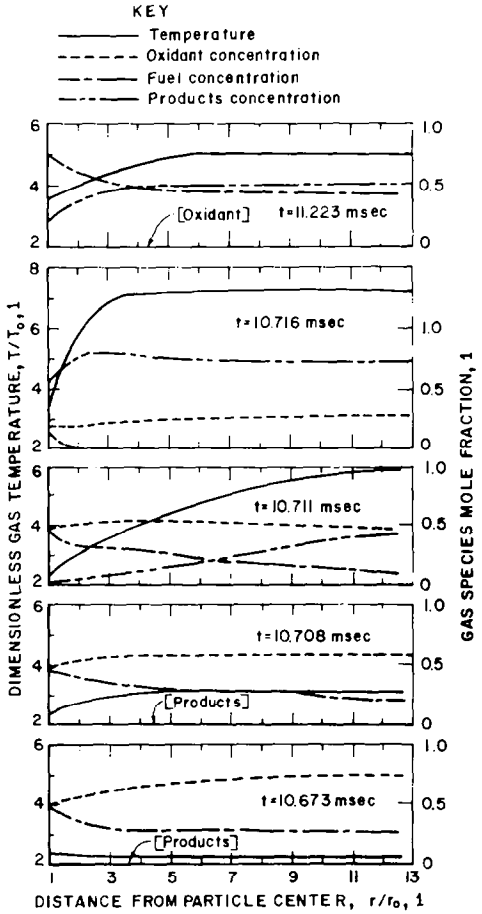

FIG. 2. The gas temperature and gas species profiles of a 490-mg l^{-1} coal dust flame immediately before, during, and after the gas phase ignition.

rather uniform. From time $t = 10.708$ to 10.716 msec, drastic changes have occurred not only in the temperature profiles, but also in the species molefraction profiles as well. A homogeneous ignition within the gas subsystem heated most of the gas volume, and set up a large thermal gradient 3 particle radii from the coal particle. The coal particle was rapidly heated by gas conduction thereby producing more fuel by pyrolysis to sustain the combustion. At time $t = 11.223$ msec, the gas phase combustion terminated due to the complete consumption of oxidant.

Figure 2 reveals some interesting chemical and physical phenomena. In heat diffusion processes, long length scales and timescales are usually expected. However, after the fuel–oxidant ignition, the high rate of enthalpy production established a large thermal gradient over a very short distance near the particle heating the particle at an initial rate of 24,000 cal/sec. During this ignition period, processes that had been decoupled by virtue of the widely disparate time constants had then become tightly coupled because of drastic changes in condition. From [46], parameters such as the flame temperature, dust concentration, coal particle radius, and input velocity, etc., form a complete set which has a unique solution. However, there exists a continuous family of solutions, each of which exists for a different parameter set. If the iteration process were not performed carefully, i.e., Kantorovich's theorem were violated, then the iteration process could jump to a different solution branch which was not part of the original parameter set. Smoot and Horton [47] in their coal dust calculations also reported the existence of multiple solutions, some of which were not physically realized, if their time step selection and iteration parameters were improperly chosen.

Shampine and Gear [48] evaluated the technique of removing stiffness from a model by changing the model. If certain chemical reactions attain equilibrium very rapidly, one could substitute equilibrium expressions for such reactions. However, they cite an example in which such approximations resulted in the wrong steady state.

In a recent paper, Briley and McDonald [35] recommend viewing a time marching scheme as an overall iteration scheme seeking the steady state solution (if one exists). By cyclically applying a sequence of time steps which range within physically permitted timescales, convergence to steady state was accelerated. Small time steps reduce the small spatial wavelength errors, while large time steps reduce the large spatial wavelength errors. An analogous viewpoint had been expressed earlier by Boggs [44] and Branin [49] regarding damped Newton–Raphson schemes and A-stable ODE schemes; however, without the cycling procedure. The damping parameters of the NR scheme may vary considerably, but the finest resolution was recommended for solution trajectories in regions of high nonlinearity. In dealing with combusting gasdynamic systems, the algorithm used to solve the governing PDEs should be flexible to follow the evolution of the solution trajectory in both the highly nonlinear regions as well as the nearly linear regions in the most efficient manner possible.

Kooker [19] showed that while block implicit methods are numerically stable for confined flame calculations using time steps considerably larger than the sound speed restrictions, such solutions are physically incorrect. Even though the acoustic

pressure interaction accelerates the flame front giving no steady state solution, he has found that a linearly stable block implicit code does not, per se, guarantee physical correctness unless the proper deterministic time step based on the burnt gas sound speed is used. His results should stimulate the analyst to examine his solution technique, to formally verify his results and understand his conclusions.

Branin [49] has studied the problem of solving systems of nonlinear equations and the location of multiple solutions. Using a damped Newton method with a steering correction, he has found that if too large a Newton step is taken, the trajectory may pass over several solution points of $\Psi(\Phi) = 0$ if they happen to be closely connected. He recommends computing the orthogonal component of the vector as a function of the distance along the trajectory. If this orthogonal component increases too rapidly, then smaller changes are required. Also there is danger if the Jacobian changes sufficiently without updating in severely nonlinear regions. The regions described by the loci of singular Jacobians were observed to be saddle and vortex points. His recommendations were incorporated into the algorithm, especially for the highly nonlinear, exothermic ignition processes.

The analysis of multiple steady states that are possible from the deterministic equations was provided by Andronov *et al.* [50]. The steady states of large fires in vertical shafts are classified as bistable; a combusting steady laminar flow which suddenly switches to a turbulent flame is classified as a metastable steady state. In addition, Mangel [51] has provided a simple example illustrating multiple steady states that could be obtained in a finite difference scheme. Consider the differential equation

$$dx/dt = (x-1)\cdot(x-3)\cdot(a-x), \tag{72}$$

where $x(0) < 1$ and $1 < a < 3$. The stable steady states are $x = 1$ and $x = 3$, while $x = a$ is an unstable steady state. However, $x = 1$ is the true steady state given the initial condition, $x(0) < 1$. If this differential equation, Eq. (72), is integrated by a finite difference scheme, it is possible to end up at the steady state solution $x = 3$ if the time steps are too large. To miss the proper steady state at $x = 1$, suppose that $x(t) < 1$ and $x(t + \Delta t) > a$. If the time step, $\Delta t > 1/|(x-1)\cdot(x-3)|$ were used, then the finite difference scheme will yield $x = 3$ the steady state solution, instead of $x = 1$ which is the true solution. Mangel [52] also constructed a theory for predicting the probability that a nonlinear system may be driven to a multiple steady state, $P2$, by fluctuations against the deterministic flow starting from an initial state which is deterministically attracted to the steady state, $P0$. He further discusses the misuse of mathematics corresponding to linear dynamics when the dynamics are totally nonlinear.

VII. Computational Efficiency Considerations

This section will compare the computational efficiency of the iterative BI-ADI scheme with simpler approaches. Also the problem of efficiently solving a large

system of PDEs by the BI-ADI scheme for detailed chemical kinetics will be discussed.

In both the stiff ODE and PDE schemes, the nonlinear PDEs are linearized by some variation of the Newton method. The resulting linear equations are solved, in general, most efficiently by direct methods. However, the direct algorithms specifically designed for tridiagonal and block tridiagonal are more efficient than the general purpose Gaussian elimination procedure. Although simpler schemes do exist for solving linear and nonlinear equations, ODEs and PDEs, not all schemes are equally efficient and robust.

Suppose a two-dimensional combusting fluid flow problem is considered having L coupled equations and N grid points along each coordinate axis. In addition, suppose that the problem is characterized by a very large exothermic chemical enthalpy production rate, so that for a reasonable time step the nonlinear truncation errors are greater than the temporal truncation errors justifying an iterative block implicit-ADI scheme. Furthermore, assume the worst possible case in which an updated Jacobian is required for each iteration along each ADI sweep. Two traditional schemes, the iterative uncoupled Crank–Nicholson and the ICE-like RICE and APACHE schemes, will be compared on an operational count with the iterative block implicit-ADI scheme. A conservative estimate of the operation count of the ICE-like schemes is $2LN^2$; the operation count for the iterative uncoupled Crank–Nicholson scheme which gives rise to a simple tridiagonal matrix is $2NL(10N-8)$. On the other hand, the operation count for the iterative block implicit-ADI scheme per iteration is $2N(3N-2)L^2(L+1)$. To compare the relative efficiencies of each scheme, suppose that in solving the above problem the same time step and error criterion for convergence is imposed on each scheme. The iterative block implicit-ADI scheme is said to be more efficient if this scheme converges within a prescribed error tolerance using fewer operations.

$$I_{\mathrm{IBI}} \leqslant (10N-8)\, I_{\mathrm{CN}}/[L(L+1)(3N-2)], \tag{73}$$

$$I_{\mathrm{IBI}} \leqslant N I_{\mathrm{ICE}}/[L(L+1)(3N-2)]. \tag{74}$$

For example, if $L=6$ and $N=20$, the iterative block implicit scheme must converge approximately 13 times faster than the decoupled Crank–Nicholson scheme and 126 times faster than the ICE schemes. Ramshaw and Dukowicz [6] in discussing the APACHE code state that in problems with large amounts of heat release, 500 or more iterations per time step may be required for convergence, if indeed it occurs at all. In order for the IBI-ADI scheme to be more efficient than the APACHE code, it must converge within 4 iterations, which is the normal case.

If the physical processes in combusting flow problems such as gas explosions in coal mine corridors are of primary interest, then five to seven conservation equations using global chemical kinetics are adequate. However, if the chemical processes are of primary interest such as air pollution control or flame inhibitor studies, then at least 30 to 50 chemical species as well as detailed chemical kinetics are required. In

detailed chemical studies, not only does computer storage become a serious problem, but also the number of operations to decompose a large block tridiagonal matrix rises astronomically. Consequently, a combination of direct and indirect methods based upon block decomposition must be considered.

Steger [53] found that the computational effort could be markedly reduced if the block of L equations were made reducible (uncoupled) by similarity transformations. He considered a two-dimensional nonreacting inviscid problem; under an appropriate similarity transformation, the original 4×4 block problem was reduced to a sequence of a 2×2, and two 1×1 problems. When complex chemically reacting systems that include Arrhenius kinetics and various forms of physical diffusion are considered, such a transformation might not exist or it may be very difficult to construct. Most likely, approximate decoupling based on chemical and physical arguments (such as grouping reactants into sets in which the timescales of transport and kinetics are either similar or dissimilar) rather than on rigorous mathematics might be the best one could expect. Briley and McDonald [35] have discussed reduction techniques such as "order epsilon decoupling" and the use of exact and approximate decoupling procedures based on chemical knowledge to simplify complex chemical problems.

The analyses of Westbrook and Haselman [54] on the detonability of natural gas (90% methane, 5–8% ethane, plus other complex hydrocarbons) are useful in gaining insight for block splitting the chemistry. Using 27 species and 75 separate chemical reactions, their analyses showed that the detonability of natural gas was primarily due to the presence of ethane which provided the source of readily available atomic hydrogen necessary to initiate the branching chain reactions. The intermediate species such as formaldehyde, molecular hydrogen, and carbon monoxide liberated very little energy so that the temperature and pressure of these reactants remain relatively unaffected. Most of the energy release comes from the oxidation of carbon monoxide and hydrogen into carbon dioxide and water, respectively, neither of which occurs significantly until near the end of the chemical induction period.

Each reaction step is controlled by the availability of free radicals. Atomic hydrogen reacts rapidly with O_2 to produce O and OH free radicals which form the core of the branching chain reactions which consume the fuel and generate more atomic hydrogen. The C–H bonds of methane which are quite strong in comparison to ethane commence bond breaking collisions in substantial numbers only after a significantly high temperature is reached.

A three-dimensional BI-ADI code with the detailed chemistry of Westbrook and Haselman [54] would be untractable on most computer systems. However, a standard technique for handling very large matrix problems is matrix partitioning, cf. Westlake [55], and can be readily applied to a block tridiagonal matrix structure. For increased efficiency, it is recommended that such partitioning be based on chemical and physical judgment.

It is suggested that the kinetic scheme for natural gas could be solved iteratively as a sequence of smaller problems. Using Westbrook and Haselman's [54] data and analysis, it appears that ethane and its daughter species would be one subgroup,

methane and its daughter species would be another, CO, H_2CO, and H_2 and heavier intermediate species would form a third group, while H, O, OH form a fourth group: H_2O and CO_2 form a fifth group; and, the mass, momentum (along a given coordinate), and energy form the last group.

Species should be grouped as much as possible according to the activation energy of the "dominant" reaction as well as the expected concentration levels based upon judgment of chemical and physical insight. The strategy of combining direct and indirect methods within an overall matrix partitioning scheme is recommended by authors such as Westlake [55] in dealing with large sets of linear and nonlinear equations.

If the finite difference scheme has been properly formulated and if the proper time steps are carefully chosen, it has been found that two to three iterations are required for convergence within some error tolerance, i.e., 10^{-6}. This present study concurs with the conclusions of Keller [10] that if more than five iterations are required, then more than likely, the numerical scheme has been improperly formulated. Because the class of Newton-like schemes converges quadratically as opposed to the linearly converging method of successive substitutions, the simpler scheme may often require more arithmetic operations than the more power Newton-like schemes.

VIII. Results of a Two-Dimensional Calculation

The algorithm developed in this paper was applied to the time evolution of a two-dimensional burning wick in a gravitational field going to steady state. A previous one-dimensional transient calculation by Hertzberg *et al.* [56] of combustion involving a spherical wick in the absence of gravity showed that the combustion eventually was extinguished because the process choked itself. Because the combustion products accumulated around the wick with no process other than diffusion to remove them, the combustion process eventually ran down because oxidant and fuel had to diffuse over increasingly larger distances in order to react, and the rate of heat loss from the combustion zone was eventually greater than the rate of exothermic heat production.

Kumagai and Isoda [57] also performed a series of photographic experiments by using an enclosed falling chamber in which fuel drops attached to a wick were ignited. After 0.3 sec of free fall, $g_{eff} = 0$, there was a considerable diminution of luminosity of the combusting fuel drop. In addition, the combustion zone as defined by the region of luminosity was considerably broadened while preserving its spherical shape. In contrast, at 0.3 sec, the full g case appeared to have been in a steady state condition for a while and the combustion region whose luminous zone assumed a teardrop shape was very intense. In addition, the luminous zone was thin at the bottom and thickened at the top.

In both the one- and two-dimensional burning spherical wick calculations, the chemical reaction describing the combustion process was an irreversible second-order reaction of "fuel vapor" and "oxidant" going to "combustion products." The

TABLE I

Parameters Used in Burning Wick Calculation

$a_{p_1} = a_{p_2} = 2.6.10^{10}$ cm^3 g^{-1} sec^{-1}
$a_{p_3} = -2a_{p_1}$
$c_{p_1} = c_{p_2} = c_{p_3} = 0.23$ cal g^{-1} K^{-1}
$D_{1,2} = D_{1,3} = D_{2,3} = 0.22$ cm^2 sec^{-1}
$E_{a_1} = E_{a_2} = E_{a_3} = 18{,}000$ cal mole^{-1}
$g = 980$ cm sec^{-2}
$K = 2.9325 \times 10^{-6} T^{1.75}$ cal cm^{-1} sec K^{-1}
$M_1 = M_2 = M_3 = 30$ g mole^{-1}
$p = 1$ atm
$R = 1.9869$ cal mole^{-1} K^{-1}
$T_0 = 300$ K
$\gamma = 1.4$
$\Delta H = 94{,}000$ cal mole^{-1}
$\mu = 1.13355 \times 10^{-5} \sqrt{T}$ poise
$\rho_0 = 1.2186 \times 10^{-3}$ g cm^{-3}

activation energy, pre-exponential constant, heat of reaction, and other system properties are summarized in Table I.

In both the one- and two-dimensional burning wick calculations, the following boundary conditions were identical: at the wick surface, $r = 1$ cm and for all angles

$$\rho_{\text{oxid}} = \rho_{\text{prod}} = 0; \qquad \rho_f = M_f/RT_{\text{boil}}; \qquad T = T_{\text{boil}} = 300 \text{ K},$$
$$\rho u = |D_{f,o}\rho\nabla(\rho_f/\rho)|; \qquad \rho v = 0. \tag{75}$$

The burning wick and oxidant were enclosed in a large mathematical volume of radius 80 cm. At this boundary, the conditions that apply are

$$P = 1 \text{ atm}; \qquad T = 300 \text{ K},$$
$$\rho_f = \rho_{\text{prod}} = 0, \tag{76}$$
$$\rho_{\text{oxid}} = M_{\text{oxid}}/RT.$$

The initial conditions for both sets of calculations were: constant and uniform pressure, no gas motion, and a uniform temperature distribution at 300 K everywhere except for an ignition region set at 2250 K 2 cm from the wick. Furthermore, the oxidant density was uniform for all radii greater than 2 cm; the fuel density, for all radii less than 2 cm. The initial conditions are (for all angles):

$$\rho u = \rho v = 0 \text{ for all } r > 1 \text{ cm}; \qquad \rho_{\text{prod}} = 0 \text{ for all } r \geqslant 1 \text{ cm},$$
$$P = 1 \text{ atm for all } r, \tag{77}$$

$$T = 300 \text{ K for all } r = 2 \text{ cm}, \qquad T = 2250 \text{ K for } r = 2 \text{ cm};$$
$$\rho_f = M_f/RT \text{ for } r \leqslant 2 \text{ cm}; \ \rho_f = 0 \text{ for } r > 2 \text{ cm}. \tag{78}$$

The problem of using an adequate mesh to best resolve the diffusion flame surrounding the sperical wick was resolved by numerical experimentation. The radial coordinate was spanned by an exponentially stretching coordinate system with the finest resolution. The radial coordinate was stored as a vector whose form is given by

$$r(j) = exp(\Delta Z \cdot (j-1)), \tag{79}$$

where

$$\Delta Z = \frac{\log(80.0)}{(24-1)} = 0.19052.$$

This problem was deemed adequately resolved by such a radial grid because unlike a propagating laminar premixed flame, this flame is essentially a stationary diffusion-like flame. In the half plane, $0 \leqslant \Theta < \pi$, the angular coordinate was spanned by a uniform mesh of 10 points. The other half plane was generated by symmetry considerations.

The RICE [4, 5] and APACHE [6] codes provide the details of the governing PDEs in conservative form. For completeness the conservation equations and finite difference approximations are given in Appendix B. The vector of the residuals and the Jacobian for the radial and angular sweeps can be reconstructed in a straightforward manner.

At $t = 0$, there were large temperature and concentration gradients at $r = 2$ cm. As molecular diffusion and thermal conduction smooth the profiles to cause a sufficient overlap of the fuel and oxidant, the second-order Arrhenius reaction commences to produce heat and product gases. The combustion wave flows both outward to infinity and inward to the spherical wick. Both convection and diffusion mix oxidant and fuel, thereby increasing the combustion rate.

This initial combustion phase occurred on less than a millisecond timescale. However, as the hot combustion zone thickens, the rate of combustion and heat release gradually slows down because fuel and oxidant must diffuse over increasingly larger distances before they can react. During the first 200 msec, the velocity vectors and the temperature contours are overwhelmingly radial and symmetric, cf. Fig. 3. (In both Figs. 3 and 4, the gravitational acceleration is directed downward; since the radius of the wick is 1 cm, the lengths may be estimated by referring to the figures.) During this period, the maximum gas velocity is about 250 cm/sec which corresponds to a flame speed of about 290–310 cm/sec.

As time evolves, there is a slow steady departure from spherical symmetry due to the buoyant force. Buoyancy aids in the removal of combustion products near $\theta = \pi$, thereby narrowing the distance over which oxidant and fuel must diffuse in order to react. Eventually the flow field and the temperature distribution will no longer exhibit spherical symmetry.

Figure 4 shows the immediate flow field over the spherical wick and the temperature profiles 1.2 sec after ignition. The maximum initial temperature was 2250 K, but it has now dropped to 2100 K. In the upper half of Fig. 4, the combustion zone is considerably thicker than that in the lower half plane. The

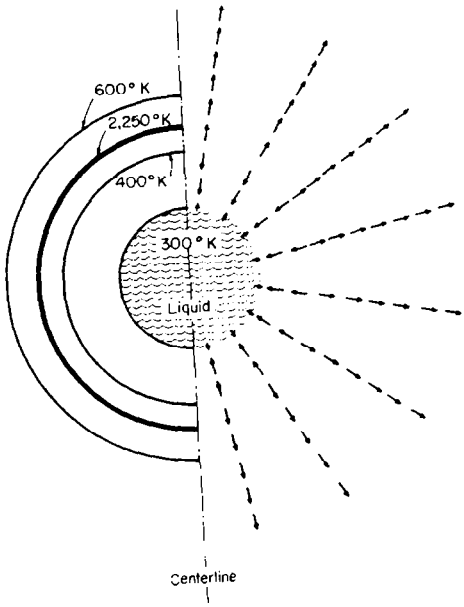

FIG. 3. The convective gas flow and temperature contours of a burning spherical wick in a gravitational field 50 msec after ignition.

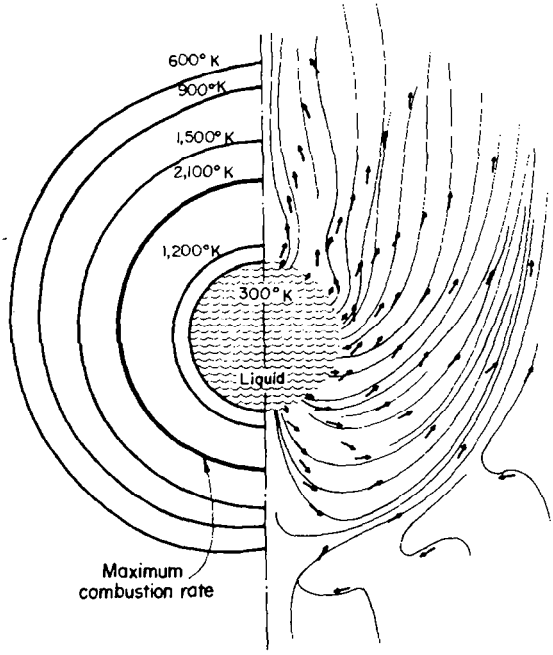

FIG. 4. The convective gas flow and temperature contours of a burning spherical wick in a gravitational field 1.2 sec after ignition.

oxidant in the upper half plane near $\theta = 0$ has been considerably diluted by product gases which were convected there by buoyancy. In addition, there is a preferential region, near $\theta = \pi$, for combustion to occur because fresh oxidant is constantly being supplied and hot product gases are constantly being swept away by buoyancy forces.

The flow field (on the order of 4 cm/sec) is no longer predominantly radial, but exhibits a considerable amount of tangential flow. The flow profile shows that cold oxidant flows down toward the bottom of the wick, then upward to react with the fuel vapor. In the temperature region, 600–1500 K, the flow pattern is directed upward indicating that hot product gases are being convected upward from $\theta = \pi$ to $\theta = 0$ by the buoyantly induced convection. This picture agrees well with the photographic evidence of Kumagai and Isoda [57] and the analysis of Hertzberg *et al.* [58]. In addition, the quantitative agreement of the maximum velocities of the flow field during both the ignition and steady state phases is in excellent agreement with observation. A more complete study of the influence of buoyancy upon combustion will appear in a separate paper.

During the rapid combustion phase, time steps on the order of 0.1 msec were used. The burnt gas sound speed is approximately 94,500 cm/sec. Such a time step is about 470 times greater than the explicit CFL time step. During this transient phase, the Jacobian was updated often in the radial sweep (the approximate updating modules of Broyden and Powell required too much computer memory); as much as three iterations were required per time step in the radial ADI sweeps.

The PDEs were cast into dimensionless form; the diffusion coefficients were rather small in comparison to the pressure and enthalpy of combustion. To prevent numerical diffusion from becoming too large, the numerical diffusion was restricted to be less than 2% of the actual physical diffusion. The value of the time splitting parameter was taken to be $\Theta = \frac{1}{2} + 1.5 \times 10^{-7}$. Of course, in other problems, this amount varies with the scaling parameters.

As the burning wick system slowly evolved toward the steady state configuration, time steps of approximately 10 msec were used which is 20% of the maximum convective time step restriction. In this stage, the rate of enthalpy production by combustion is being controlled by the buoyantly induced convection and molecular diffusion. Since the radial and tangential momentum components are comparable in magnitude, convergence was achieved in one iteration during both the radial and tangential ADI sweeps. It might be said that the conditions during the approach to steady state are very favorable for very large time steps. In this stage, the time step is on the order of the convective limit; but it was chosen more cautiously to minimize large changes in the temperature which would affect the Arrhenius kinetics. Note that this more cautious approach was also taken by Lund [20]. During the highly transient stage, based on an approximate operation count, an explicit calculation would be comparable in effort to the iterative block implicit-ADI scheme. However, as steady state is approached, block implicit methods become significantly more efficient than explicit schemes.

During the highly transient initial ignition period, the radial momentum component should overwhelm the tangential component. This information was not exploited, and the six conservation equations (one mass, one energy, two momenta, and two species) were not decoupled. The matrix inversions of the 6×6 matrix required for the tridiagonal block decomposition scheme were handled by a double precision subroutine. Lund [20] showed that a considerable gain in computational efficiency could be realized if the matrix handling routines were done in assembly language routine, rather than by a Fortran routine. This run took about 6.5 hr on a Burroughs 6700 computer; this time appears to be competitive according to Otey [22] who tested other PDE solvers.

This method is also being applied to a 3-phase problem of wood and coalbed combustion in which a very nonlinear water evaporation and condensation source term as well as a three step global pyrolysis scheme is included. Block reduction techniques are being used in those temperature regimes where it is known that certain reactions are decoupled.

An interesting experiment verifying the predicted results of these calculations would be to conduct a burning wick experiment aboard a satellite in a free falling orbit about Earth. The calculations predict that in the absence of gravitational acceleration, a spherical burning wick would eventually extinguish because the combustion process would choke itself. However, in an accelerating field, buoyancy induces an asymmetric flow field by which cold oxidant is being supplied to support the combustion at the bottom while hot product gases are being swept away at the top.

SUMMARY

The algorithm presented in this paper is a complex strategy designed to solve highly transient, highly nonlinear multidimensional PDEs which occur during highly exothermic combusting gas dynamics. It has built upon the earlier works of Briley and McDonald [12] and Beam and Warming [13] who devised an efficient noniterative block implicit-ADI scheme for multidimensional fluid flow problems. However, when dealing with highly exothermic combusting gas dynamics with Arrhenius chemical kinetics, the noniterative block implicit-ADI scheme will not be sufficient for all such problems. Because of the complications introduced by considering highly exothermic combustion with Arrhenius kinetics, the basic strategies that worked well with the stiff Gear-like ODE and nonlinear equation solvers were adopted in this algorithm; i.e., the implicit treatment of the FDEs, the use of Newton-like methods to solve the resulting FDEs, and dynamic step length control, or damping of the NR corrections. Care was taken in highly nonlinear regions to ensure that solution trajectory did not branch to a spurious solution. Iteration is used only if the norm of the residual errors of the FDEs exceeds a given error tolerance. According to linear theory, an implicit formulation of a set of PDEs is unconditionally stable provided that system only involves convection and diffusive

approach, but it is advisable to continuously determine which method is best suited for a given set of circumstances.

The decision whether to use implicit or explicit schemes, as seen from Kooker's findings, appears to be quite problem dependent. A conservative approach would be to choose an explicit scheme if q_{chem} is quite small in comparison to energy transport, and if the convective flow is above 0.05 Mach. Because an operation count is about the only simple heuristic manner in which to make such a decision, an explicit scheme is more efficient in a time interval t_1 to t_2, if the expected number of operations from an explicit scheme is less than that of either an iterative or noniterative BI scheme.

However, as a general rule, implicit schemes are increasingly more efficient with increasing spatial resolution. Fasel [60] has compared the relative efficiency, based on an operation count, of explicit and implicit schemes with increasing spatial resolution. He concludes that there exists a crossover point at which implicit schemes become increasingly more efficient than explicit schemes as the spatial resolution increases.

Combustion also offers an additional complication because of the possibility of multiple solutions (cf., Branin [49], Mangel [51, 52], Ortega and Rheinboldt [37], and Lewis and von Elbe [61]). By properly formulating the solution procedure to ensure each part of Kantorovich's conditions are met (monitoring Δt, the Jacobian and convergence of Ψ), Kantorovich's theorem guarantees convergence to a unique solution, Φ^{n+1}, at every step.

The comments of Shampine and Gear [48] for ODE solvers apply equally well for PDE solvers. All such codes are problem dependent and require fine tuning for efficiency. Some codes developed for one class of problems may turn out to be inefficient for other classes of problems. They also caution about using time steps so large than an active component of the solution is missed. They emphasize the need for a conservative choice of error tolerance and scaling, experimentation, and thoughtful examination of the numerical results.

APPENDIX A: SUMMARY OF STRATEGIES

The desired goal in solving systems of multidimensional PDE problems is to obtain reliable results at the minimum of cost. As pointed out in several references regarding stiff ODEs and nonlinear equations, there is no comprehensive mathematical theory developed to date to solve such problems in the most efficient manner. The optimal strategy is problem dependent, and fine tuning and experience are required. Other than experience, an operational count can help one decide which path is the most efficient at a given time.

I. Initialize problem, $t = 0$.

II. Estimate timescales, pick smallest to start problem.

III. $t^{n+1} = t^n + \Delta t$.

IV. Explicit–implicit operations count, assume

$$\Delta t_{\min} \leqslant \Delta t_{\text{expl}} \leqslant \Delta t_{\text{impl}}.$$

A. Is $N_{\text{op}}(\text{expl})\,\Delta t_{\text{expl}} < N_{\text{op}}(\text{impl})\,\Delta t_{\text{impl}}$?

1. Yes. Is transport slow in comparison to chemistry? If so, choose implicit chemistry, explicit hydro solver (cf. Westbrook and Haselman [54]).
2. No. To optimize efficiency in most cases choose BI-ADI scheme (cf. McDonald [26]).

V. BI-ADI scheme.

A. Noniterative BI-ADI scheme ($ITR = 1$).

1. Construct Ψ.
2. Use old J and its decomposition if available.
3. Obtain $\delta\Phi(1)$ and $\Phi^{n+1}(1)$.
4. Test whether $\| \Psi(\Phi^{n+1}(1))\| < \varepsilon$.
5. If yes, increase time step, go to III.
6. If no, go to V.B.

B. Iterative BI-ADI scheme.

1. Check Jacobian conditioning.
   Is $\min_i\{I + \Delta t\, \Theta\, \partial H/\partial\Phi\}_{ii} > 0$?
2. If no, pick Δt which satisfies above restriction, reinitialize Φ^{n-1}, go to III.
3. If yes, determine whether reducing Δt is more efficient than reducing nonlinear truncation errors by iteration.
   a. Hopeless-case-runaway divergence if $\|\delta\Phi(1)\| > M\eta$ and $\|\Psi(1)\| > M\varepsilon$ ($M \sim 10^4 \sim 10^5$), flag divergence, reduce Δt, reinitialize Φ^{n-1}, go to III.
   b. Possibly converged case $\|\delta\Phi(1)\| < M\eta$; $\|\Psi(1)\| < M\varepsilon$ go to V.B.4.
4. $ITR = ITR + 1$.
   a. Use Powell's method for obtaining $\delta\Phi(ITR + 1)$.
   b. Check if $\|\Psi(ITR + 1)\| < \varepsilon$.
      (i) If yes, go to III.
      (ii) If no, go to V.B.4.
   c. Check whether

$$\|\Psi(ITR + 1)\| < \|\Psi(ITR)\|,$$

$$\|\delta\Phi(ITR + 1)\| < \|\delta\Phi(ITR)\|.$$

   d. If yes, go to V.B.4 if $ITR < ITR\ MAX$; otherwise, go to V.B.5.
   e. If no, update J, J^T, and J^{-1} (i.e., decomposition).
      (i) If J is well conditioned, and if

$$ITR < ITR\ MAX,$$

go to V.B.4.

(ii) If J is not well conditioned, adjust Δt, reinitialize Φ^{n+1}, go to III.

5. $ITR = ITR\ MAX$.

$$\| \Psi(ITR\ MAX) \| > \varepsilon.$$

The time step is too big, reduce Δt, reinitialize Φ^{n+1}, go to III.

VI. $t = T_{\max}$. Stop calculation.

APPENDIX B: CONSERVATION EQUATIONS

The problem of the burning wick is done in spherical geometry assuming azimuthal symmetry. The conservation equations are found in RICE [4], and in the standard reference by Bird *et al.* [62]. To obtain the momentum equations in conservative form, take the momentum equation given by Bird, and add to it the mass conservation equation multiplied by the appropriate velocity component.

To simplify the energy equation, it was assumed that all the diffusion coefficients, specific heats, and molecular weights were constant and equal for each species.

For programming simplicity, the following compact vector notation was used.

$$\Phi = [\rho, mr, mt, e, \rho_o, \rho_f]^T,$$

$$\mathbf{CR} = [1, ur, vt, (p+e)/\rho, X_f, X_o]^T,$$

$$\mathbf{F} = CRmr,$$

$$\mathbf{CT} = [1, ur, vt, (p+e)/\rho, X_f, X_o]^T,$$

$$\mathbf{G} = \mathbf{CT}mt,$$

$$\mathbf{PR} = [0, p, 0, 0, 0, 0]^T, \qquad \mathbf{PT} = [0, 0, p, 0, 0, 0]^T,$$

$$\frac{\partial JR}{\partial r} = \left[0, \frac{\partial ur}{\partial r}, \frac{\partial vt}{\partial r}, \frac{\partial T}{\partial r}, \frac{\partial X_f}{\partial r}, \frac{\partial X_o}{\partial r}\right]^T,$$

$$\frac{\partial JT}{\partial \theta} = \left[0, \frac{\partial ur}{\partial \theta}, \frac{\partial vt}{\partial \theta}, \frac{\partial T}{\partial \theta}, \frac{\partial X_f}{\partial \theta}, \frac{\partial X_o}{\partial \theta}\right]^T,$$

$$\sigma = \begin{bmatrix} 0 \\ \mu \\ \mu \\ k \\ \rho D \\ \rho D \end{bmatrix};$$

$$\mathbf{S} = \left[0, \left\{-\rho g \cos\theta - \frac{mtvt}{r} + \mu\left[\frac{2ur}{r^2} + \frac{2}{r}\frac{2vt}{\partial\theta} - \frac{2vt\cot\theta}{r}\right]\right\},\right.$$

$$\left.\left\{\rho g \sin\theta + \frac{mrvt}{r} - \frac{\mu vt}{r^2\sin\theta}\right\}, \{\Delta H_c \dot{\omega}_{\text{prod}} + VIS.ENG\}, \dot{\omega}_f, \dot{\omega}_o\right]^T,$$

where

$$ur = mr/\rho, \qquad vt = mt/\rho, \qquad X_f = \rho_f/\rho, \qquad X_o = \rho_o/\rho,$$

$$e = \rho E = c_v \rho T + \tfrac{1}{2}(mr^2 + mt^2)/\rho,$$

$$p = (\gamma - 1)[e - \tfrac{1}{2}(mr^2 + mt^2)/\rho],$$

$$T = \frac{1}{c_v}\left[e/\rho - \tfrac{1}{2}(ur^2 + vt^2)\right]$$

$$VIS.ENG = 2\mu\left[\left(\frac{\partial ur}{r}\right)^2 + \left(\frac{1}{r}\frac{\partial vt}{\partial\theta} + \frac{ur}{r}\right)^2 + \left(\frac{ur}{r} + \frac{vt\cot\theta}{r}\right)^2 + \left[\frac{r\partial}{\partial r}\frac{(vt)}{r} + \frac{1}{r}\frac{\partial ur}{\partial\theta}\right]^2 - \frac{1}{3}\left[\frac{1}{r^2}\frac{\partial}{\partial r}(r^2 vr) + \frac{1}{r\sin\theta}\frac{\partial}{\partial\theta}(vt\sin\theta)\right]^2\right].$$

The chemistry is a one step irreversible bi-molecular reaction given by

$$o + f \rightarrow \text{products},$$

$$\dot{\omega}_p = -\dot{\omega}_o = -\dot{\omega}_f,$$

$$\dot{\omega}_o = \dot{\omega}_f = A_p \exp(-E/RT)\,\rho_o \rho_f.$$

The six conservation equations can then be expressed compactly as

$$\Psi = \frac{\partial\Phi}{\partial t} + \frac{1}{r^2}\frac{\partial}{\partial r}(r^2 CRmr) + \frac{1}{r\sin\theta}\frac{\partial}{\partial\theta}(\sin\theta CTmt) - \frac{1}{r^2}\frac{\partial}{\partial r}\left(r^2\sigma\frac{\partial JR}{\partial r}\right) - \frac{1}{r^2\sin\theta}\frac{\partial}{\partial\theta}\left(\sin\theta\sigma\frac{\partial JT}{\partial\theta}\right) + \frac{\partial P}{\partial r} + \frac{1}{r}\frac{\partial P}{\partial\theta} + S = 0.$$

For convenience, define a exponentially stretching coordinate system

$$r = e^z$$

so that

$$\frac{\partial}{\partial r} = \frac{1}{r}\frac{\partial}{\partial z},$$

Ψ is recast as

$$\Psi = \frac{\partial \Phi}{\partial t} + \frac{1}{r^3}\frac{\partial}{\partial z}(r^2 CRmr) + \frac{1}{r \sin\theta}\frac{\partial}{\partial \theta}(\sin\theta CTmt) + \frac{1}{r}\left[\frac{\partial PR}{\partial z} + \frac{\partial PT}{\partial \theta}\right]$$

$$- \frac{1}{r^2}\frac{\partial}{\partial z}\left(r\sigma\frac{\partial JR}{\partial z}\right) - \frac{1}{r^2 \sin\theta}\frac{\partial}{\partial \theta}\left(\sin\theta\sigma\frac{\partial JT}{\partial \theta}\right) + S = 0.$$

Because finite difference schemes may give rise to truncation errors which behave as negative diffusion, such terms are cancelled by the method report by Rivard *et al.* [4]. These terms are accounted for by adding extra positive diffusion to the physical diffusion terms and in the source terms, cf. Appendix C.

The finite difference equations have all the variables centered about the point r_i, θ_j or (Z_i, θ_j).

The trapezoidal rule for the time marching scheme is expressed as

$$\Psi = \Phi_{ij}^{n+1}(k) - \Phi_{ij}^{n} + \Delta t\,\theta H_{ij}(\Phi_{ij}^{n+1}(k)) + \Delta t(1-\theta)\,H_{ij}(\Phi^n),$$

where

$$H_{ij} = OR_{ij} + OT_{ij} + S_{ij},$$

$$\begin{aligned} OR_{ij} = 1/(r_i^3 \Delta z)\big[&\tfrac{1}{2}\{(r_{i+1}^2 CRMR)_{i+1,j} - (r^2 CRMR)_{i-1,j}\} \\ &- r_{i+1/2}^2 \varepsilon r_{i+1/2,j}^{+}((CRMR)_{i+1,j} - (CRMR)_{i,j})/2 \\ &+ r_{i-1/2}^2 \varepsilon r_{i-1/2,j}^{-}((CRMR)_{i,j} - (CRMR)_{i-1,j})/2 \\ &+ (1/\Delta Z)\{r_{i+1/2}\sigma_{i+1/2,j}[JR_{i+1,j} - JR_{i,j}] \\ &- r_{i-1/2}\sigma_{i-1/2,j}[JR_{i,j} - JR_{i-1,j}]\} \\ &+ 1/(2r\,\Delta Z)(PR_{i+1,j} - PR_{i-1,j})\big]. \end{aligned}$$

If $\sin\theta_j \neq 0$, then

$$\begin{aligned} OT_{i,j} = 1/(r_i \sin\theta\,\Delta\theta) \cdot \big\{\big[&\tfrac{1}{2}((\sin\theta CTMT)_{i,j+1} - (\sin\theta CTMT)_{i,j-1}) \\ &- \sin\theta_{j+1/2}\varepsilon t_{i,j+1/2}^{+}((CTMT)_{i,j+1} - (CTMT)_{i,j})/2 \\ &+ \sin\theta_{j-1/2}\varepsilon t_{i,j-1/2}^{-}((CTMT)_{i,j} - (CTMT)_{i,j-1})/2 \\ &- (1/(r_i\,\Delta\theta)) \cdot [(\sigma\sin\theta)_{i,j+1/2}[JT_{i,j+1} - JT_{i,j}] \\ &- (\sigma\sin\sigma)_{i,j-1/2}[JT_{i,j} - JT_{i,j-1}]]\big\} \\ &+ (1/r\,2\Delta\theta)[PT_{i,j+1} - PT_{i,j-1}]. \end{aligned}$$

If $\sin\theta_j = 0$, then

$$\begin{aligned} OT_{ij} = 2/(r_i\,\Delta\theta) * \{[\tfrac{1}{2}((CTMT)_{i,j+1} - (CTMT)_{i,j-1}) \\ - \varepsilon t^{+}_{i,j+1/2}((CTMT)_{i,j+1} - (CTMT)_{i,j}) \\ + \varepsilon t^{-}_{i,j-1/2}((CCTMT)_{i,j} - (CTMT)_{i,j-1}) \\ - (1/r_i\,\Delta\theta)|\sigma_{i,j+1/2}[JT_{i,j+1} - JT_{i,j}] \\ - \sigma_{i,j-1/2}[JT_{i,j} - JT_{i,j-1}]\}| \\ + (1/2r_i\,\Delta\theta)[PT_{i,j+1} - PT_{i,j-1}]. \end{aligned}$$

$$\varepsilon r_{\pm} = \Delta t/2r_i\,\Delta Z[ur_{i,j} + ur_{i\pm i,j}].$$

$$\varepsilon t_{\pm} = \Delta t/2r_i\,\Delta\theta[vt_{i,j} + vt_{i,j\pm 1}].$$

The Jacobian has a block tridiagonal structure for either the r or θ sweep. Terms involving ur, vt, T, p, X_f, X_o in the Jacobian are related to the conservative variables in Φ by the chain rule.

APPENDIX C: Temporal Truncation Errors

The time marching scheme considered is the trapezoidal rule of maximum order 2. Even though the amount of implicitness is controlled by the parameter Θ, an exact second-order scheme could still give rise to destabilizing truncation errors from the higher-order terms. Following Rivard *et al.* [4, 5], a small controlled amount of positive numerical diffusion is retained to counter any instabilities from the neglected higher-order terms and the negative diffusion terms are cancelled. No attempt was made to control the dispersion errors.

Because the flow is known to be subsonic, all terms greater than $O(u^2)$ are neglected. The temporal truncation terms which were considered are listed as:

$$(2\Theta - 1)\frac{\Delta t}{2}\frac{\partial^2 \rho}{\partial t^2} = \frac{(2\Theta - 1)}{2}\Delta t\,\nabla\cdot[\nabla p + \mathbf{u}(\nabla\cdot\mathbf{m}) + \mathbf{u}\cdot\nabla\mathbf{m} - \mathbf{u}\mathbf{u}\cdot\nabla\rho] \qquad \text{(mass)},$$

$$\begin{aligned} (2\Theta - 1)\frac{\Delta t}{2}\frac{\partial^2 \rho^{\alpha}}{\partial t^2} = \frac{(2\Theta - 1)}{2}\Delta t\,\nabla\cdot[\mathbf{u}\mathbf{u}\cdot\nabla\rho^{\alpha} + (\rho^{\alpha}/\rho)\{\nabla p + \mathbf{u}\cdot\nabla m \\ + \mathbf{u}(\nabla\cdot m) - \mathbf{u}\mathbf{u}\cdot\nabla\rho\}] \qquad \text{(species)}, \end{aligned}$$

$$\begin{aligned} (2\Theta - 1)\frac{\Delta t}{2}\frac{\partial^2 \mathbf{m}}{\partial t^2} = (2\Theta - 1)\frac{\Delta t}{2}\Bigg[\nabla\cdot\{2\mathbf{u}\,\nabla p + 2\mathbf{u}\mathbf{u}\cdot\nabla m + \mathbf{u}\mathbf{u}(\nabla\cdot m) + \cdots\} \\ + (\gamma - 1)\nabla\left\{\gamma\mathbf{u}\cdot\nabla\varepsilon + \left(\gamma\varepsilon/\rho - \frac{(\gamma - 1)}{2}u^2\right)(\nabla\cdot\mathbf{m})\right. \\ \left. - \mathbf{u}\cdot(\mathbf{u}\cdot\nabla\mathbf{m}) + \cdots\right\}\Bigg] \qquad \text{(momentum)}, \end{aligned}$$

$$(2\Theta-1)\frac{\Delta t}{2}\frac{\partial^2\varepsilon}{\partial t^2}=(2\Theta-1)\frac{\Delta t}{2}\left[\nabla\cdot\left\{\gamma^2\mathbf{uu}\cdot\nabla\varepsilon+(\gamma-1)\frac{\varepsilon}{\rho}\nabla\varepsilon\right.\right.$$

$$+\gamma(\gamma+2)\frac{\varepsilon}{\rho}\mathbf{u}(\nabla\cdot\mathbf{m})+\gamma\frac{\varepsilon}{\rho}(\mathbf{u}\cdot\nabla\mathbf{m})$$

$$\left.\left.-\gamma(\gamma+1)\frac{\varepsilon}{\rho}\mathbf{uu}\cdot\nabla\rho\right\}+\cdots\right]\qquad\text{(energy)},$$

where

$$\mathbf{u}=\mathbf{m}/\rho,$$

$$p=(\gamma-1)\{\varepsilon-\tfrac{1}{2}(\mathbf{m}\cdot\mathbf{u})\}.$$

Although many of the terms are positive, the velocity vector and tensor, **u** and **uu**, may be negative depending upon the sign of the velocity components. For the two-dimensional spherical droplet problem with azimuthal symmetry, the operators are given by

$$\nabla=\hat{r}\frac{\partial}{r}+\frac{\hat{\Theta}}{r}\frac{\partial}{\partial\Theta},$$

$$\nabla\cdot=\frac{1}{r^2}\frac{\partial}{\partial r}(r^2)\hat{r}\cdot+\frac{1}{r\sin\Theta}\frac{\partial}{\partial\Theta}(\sin\Theta)\hat{\Theta},$$

where

$$\hat{r}\cdot\hat{r}=\hat{\Theta}\cdot\hat{\Theta}=1,$$

$$\hat{r}\cdot\hat{\Theta}=0.$$

The truncation error terms which involve mixed derivatives are treated explicitly and are lumped into the source terms. The radial and tangential derivatives are treated implicitly during the appropriate ADI sweep. After expanding the vectors, tensors, gradients, and divergences, the process of accounting for either positive or negative diffusion is straightforward but tedious.

APPENDIX D: NOMENCLATURE

a_{p_i}	the pre-exponential Arrhenius coefficient corresponding to the ith chemical reaction
A	the Jacobian matrix of the pressure and convective terms with respect to the conservative variables along the x-coordinate
B	the Jacobian matrix of the pressure and convective terms with respect to the conservative variables along the y-coordinate

CFL condition the Courant–Friedricks–Levy stability criterion for sound wave propagation in explicit hyperbolic equations, i.e., $\Delta t \leqslant x/(c + |u|_{\max})$

c_p specific heat at constant pressure (cal $g^{-1} K^{-1}$)

c_v specific heat at constant volume (cal $g^{-1} K^{-1}$)

D_{ij} multicomponent diffusion coefficient ($cm^2 sec^{-1}$)

E_{a_i} Arrhenius activation energy of ith chemical reaction (cal $mole^{-1}$)

F a column vector denoting the homogeneous form of the convective and pressure terms in conservative form for the fluxes along the x-coordinate

FDE finite difference equations

G a column vector denoting the homogeneous form of the convective and pressure terms in conservative form for the fluxes along the y-coordinate

g gravitational acceleration (cm sec^{-2})

i index subscript denoting the position x_i along the x-coordinate

I_{IBI} number of iterations required for convergence by the iterative block implicit scheme

I_{ICE} number of iterations required for convergence by the ICE-like scheme

I_{CN} number of iterations required for convergence by the decoupled Crank–Nicholson schemes

J Jacobian matrix

j index subscript denoting the position y_j along the y-coordinate

JX_x column vector denoting gradients along the x-coordinate

JY_y column vector denoting gradients along the y-coordinate

K degrees Kelvin

L number of coupled conservation equations

mr ρu_r—momentum component in radial direction

M_i molecular weight (g $mole^{-1}$)

mt ρu_t—momentum component in $\hat{\theta}$ direction

N number of spatial divisions along a coordinate axis

n superscript corresponding to the nth time step

ODE ordinary differential equations

$O_{x,y}$ the combined convective and diffusive transport operator along either the x- or y-coordinate

p pressure (atm or g $cm^{-1} sec^{-2}$)

PDE partial differential equations

$\dot{q}_{\mathrm{chem}}$ total rate of chemical enthalpy production (cal $cm^{-3} sec^{-1}$)

R ideal gas constant (cal $mole^{-1} K^{-1}$)

$\dot{R}_i$ rate of production or disappearance of the ith species

r radial distance in spherical coordinates (cm)

S column vector of the source terms

T absolute temperature (Kelvin)

t time (sec)

u gas velocity component along $x(r)$ axis

v	gas velocity component along $y(\theta)$ axis
W	column vector representing the total transport by convection and diffusion
x	spatial distance in Cartesian coordinates along x-axis (cm)
y	spatial distance in Cartesian coordinates along y-axis (cm)
α	upper bound of the norm of the inverse of the Jacobian
β	upper bound of the norm of the iterative correction vector
γ	ratio $(=c_p/c_v)$ of specific heats
$\Delta x, \Delta y, \Delta t$	finite difference increments of x, y, and t
$\delta\Phi$	iterative correction vector
$\varepsilon_{x,y}$	a dimensionless constant which varies the relative contribution of the central and upwind difference operators in spatial differencing of the convective terms
Φ	the column vector of the L dependent variable
ϕ_{ij}^n	a component of the solution vector corresponding to the time t^n and the location x_i and y_j
ζ	a dimensionless constant of Powell's algorithm
Λ	a linear matrix
λ_i	the eigenvalues of the matrix Λ
μ	a dimensionless constant of Powell's algorithm
ρ	total gas density (g cm^{-3})
ρ_i	gas density of the ith species (g cm^{-3})
π	3.14159...
$\sum$	summation operator
σ	generalized diffusion coefficients
κ	thermal conductivity (cal cm^2 sec^{-1})
Θ	a dimensionless constant which varies the degree of implicitness
θ	angular displacement in spherical coordinates
ω	norm of the Hessian matrix

ACKNOWLEDGMENTS

The author wishes to express his appreciation to Dr. Gerald Hedstrom at Lawrence Livermore National Laboratory for his helpful suggestions. This work was conducted at the U.S. Bureau of Mines Pittsburgh Research Center.

REFERENCES

1. R. O. RICHTMEYER AND K. W. MORTON, "Difference Methods for Initial-Value Problems," 2nd ed., Interscience, New York, 1967.
2. P. J. ROACHE, "Computational Fluid Dynamics," Hermose Publications, Albuquerque, N. Mex., 1972.
3. F. H. HARLOW AND A. A. AMSDEN, *J. Comput. Phys.* **8** (1971), 197.

4. W. C. RIVARD, O. A. FARMER, O. D. BUTLER, AND P. J. O'ROURKE, LA 5426-MS, LASL, October 1973.
5. W. C. RIVARD, O. A. FARMER, AND T. D. BUTLER, LASL 5812, LASL, March 1975.
6. J. D. RAMSHAW AND J. K. DUKOWICZ, LA-7427, LASL, January 1979.
7. C. WESTBROOK, *J. Comput. Phys.* **29** (1978), 67–80.
8. H. B. KELLER, *SIAM J. Numer. Anal.* **11** (1975), 179–189.
9. H. B. BRABSTON AND H. B. KELLER, *J. Fluid Mech.* **69** (1975), 179–189.
10. H. B. KELLER, *in* "Proceedings of the Fourth International Conference on Numerical Methods in Fluid Dynamics," pp. 1–21, Springer-Verlag, New York, 1975.
11. E. BAUM AND E. NEEDO, *in* "Proceedings of the AIAA Computational Fluid Dynamics Conference, New York, 1973," pp. 133–140.
12. W. R. BRILEY AND H. MCDONALD, *J. Comput. Phys.* **24** (1977), 372–397.
13. R. W. BEAM AND R. F. WARMING, *J. Comput. Phys.* **22** (1976), 87–110.
14. J. DOUGLAS AND J. B. GUNN, *Numer. Math.* **6** (1964), 42.
15. H. J. GIBELING, H. MCDONALD, AND W. R. BRILEY, AFAPL-TR-75-59, Vols. 1 and 2, 1975.
16. E. S. ORAN, T. R. YOUNG, AND J. P. BORIS, NRL Memorandum Report 3889, November 1978.
17. R. J. KEE AND J. A. MILLER, *in* "Proceedings of the 3rd AIAA Computational Fluid Dynamics Meeting, Albuquerque, New Mexico, June 1977."
18. J. S. CHANG, A. C. HINDMARSH, AND N. K. MADSEN, *in* "Stiff Differential Systems" (R. A. Willoughby, Ed.), Plenum, New York, 1973.
19. D. E. KOOKER, *in* "Seventeenth Symposium (International) on Combustion," pp. 1329–1339, The Combustion Institute, Pittsburgh, Pa., 1979.
20. C. M. LUND, UCLR-52504, LLL, August 1978.
21. H. A. DWYER, R. J. KEE, AND B. R. SANDERS, *in* "Proceedings of the Fourth Computational Fluid Dynamic Conference, July 1979." AIAA 79-1464.
22. G. R. OTEY, Sand. 78-8025, Sandia Lab., October 1978.
23. K. J. BATHE AND A. P. CIMENTO, *Comput. Methods Appl. Mech. Eng.* **22** (1980), 59–85.
24. J. K. RICHMOND AND I. LIEBMAN, *Arch. Termodynamiki Spalania* **8** (1977), 27.
25. E. J. KANSA AND H. E. PERLEE, USBM RI 8163, 1976.
26. H. MCDONALD, *Progr. Energy Combust. Sci.* **5** (1979), 97–122.
27. J. C. CHIEN, *J. Comput. Phys.* **20** (1976), 268–278.
28. T. P. BORIS AND D. L. BOOK, *J. Comput. Phys.* **11** (1973), 38–69.
29. C. W. GEAR, *Commun. ACM* **14** (1971), 176–169.
30. C. W. GEAR, *Commun. ACM* **14** (1971), 185–190.
31. M. B. CARVER, *in* "Numerical Methods for Differential Systems," (L. Lapidus and W. E. Schiesser, Eds.), Academic Press, New York, 1976.
32. R. M. BEAM AND R. F. WARMING, *AIAA J.* **16** (1978), 393–402.
33. R. M. BEAM AND R. F. WARMING, Signum Conference on Numerical ODE's, April 1979.
34. R. M. BEAM AND R. F. WARMING, *in* "Proceedings of the Fourth Computational Fluid Dynamics
36. R. J. GOULT, R. F. HOSKINS, J. A. MILNER, AND M. J. PRATT, "Computational Methods in Linear Algebra," Wiley, New York, 1974.
37. J. M. ORTEGA AND W. C. RHEINBOLDT, "Iterative Solution of Nonlinear Equations in Several Variables," Academic Press, New York, 1970.
38. B. GUSTAFSSON, *J. Comput. Phys.* **7** (1971), 239–254.
39. M. J. D. POWELL, *in* "Numerical Methods for Nonlinear Algebraic Equations," (P. Rabinowitz, Ed.), Gordon & Breach, New York, 1971.
40. A. C. HINDMARSH AND G. D. BYRNE, *in* "Numerical Methods for Differential Systems," (L. Lapidus and W. E. Schiesser, Eds.), Academic Press, New York, 1976.
41. C. G. BROYDEN, *Math. Comput.* **19** (1965), 577–593.
42. R. F. WARMING AND R. M. BEAM, *SIAM-ASM Proc.* **11** (1978), 85–129.

43. J. H. SEINFELD, L. LAPIDUS, AND M. HWANG, *Ind. Eng. Chem. Fundam.* **9** (1970), 266–275.
44. P. T. BOGGS, *SIAM J. Numer. Anal.* **8** (1971), 767–785.
45. G. G. DAHLQUIST, *BIT* **3** (1963), 27–43.
46. E. J. KANSA AND H. E. PERLEE, *Combust. Flame* **38** (1980), 17–36.
47. D. L. SMOOT AND M. D. HORTON, Final Report. J.S. Bureau of Mines, Grant G0177034, 1978.
48. L. F. SHAMPINE AND C. W. GEAR, *SIAM Rev.* **21** (1979), 1–17.
49. F. H. BRANIN. *IBM J. Res. Develop.* **16** (1972), 504–522.
50. A. A. ANDRONOV, E. A. LEONTOVICH, I. I. GORDON, AND A. G. MAIER, "Qualitative Theory of Second Order Dynamic Systems," Halsted Press, New York, 1973.
51. M. MANGEL, private communication.
52. M. MANGEL, *SIAM J. Appl. Math.* **36** (1979), 544–572.
53. J. L. STEGER, *Comput. Methods Appl. Mech. Eng.* **13** (1978), 175–188.
54. C. K. WESTBROOK AND L. C. HASELMAN, UCRL-82293, 1979.
55. J. R. WESTLAKE, "A Handbook of Numerical Matrix Inversion and Solution of Linear Equations," Wiley, New York, 1978.
56. M. HERTZBERG, K. CASHDOLLAR, C. LITTON, AND E. KANSA, Central States Meeting of the Combustion Institute, March 1977.
57. S. KUMAGAI AND H. ISODA, *in* "Sixth Symposium (International) on Combustion," pp. 726–731, The Combustion Institute, Pittsburgh, Pa., 1957.
58. M. HERTZBERG, K. CASHDOLLAR, C. LITTON, AND D. BURGESS, USBM RI 8263, 1978.
59. P. LINZ, "Theoretical Numerical Analysis," Wiley, New York, 1979.
60. H. FASEL, *in* "Computational Fluid Dynamics" (W. Kollmann, Ed.), Hemisphere Publishing Corporation, Washington, D.C., 1980.
61. B. LEWIS AND G. VON ELBE, "Combustion, Flames, and Explosions of Gases," Academic Press, New York, 1961.
62. R. B. BIRD, W. E. STEWART, AND E. N. LIGHTFOOT, "Transport Phenomena," Wiley, New York, 1960.